Using Statistical Functionals for Effective Control of Inhomogeneous Complex Turbulent Dynamical Systems

Andrew J. Majda[a], Di Qi[a,*]

[a]*Department of Mathematics and Center for Atmosphere and Ocean Science, Courant Institute of Mathematical Sciences, New York University, New York, NY 10012*

Abstract

Efficient statistical control strategies are developed for general complex turbulent systems with energy conserving nonlinearity. Instead of direct control on the high-dimensional turbulent equations concerning a large number of instabilities, a statistical functional that characterizes the total statistical structure of the complex system is adopted here as the control object. First the statistical energy equation reduces the control of the complex nonlinear system to a linear statistical control problem; then the explicit form of the forcing control is recovered through nonlocal inversion of the optimal control functional using approximate statistical linear response theory for attribution of the feedback. Through this control strategy with statistical energy conservation, the explicit form of the control forcing is determined offline only requiring the initial configuration of total statistical energy change and the autocorrelation functions in the most sensitive modes of the target statistical equilibrium, with no need of knowing the explicit forcing history and running the complex system. The general framework of the statistical control method can be applied directly on various scenarios with both homogeneous and inhomogeneous perturbations. The effectiveness of the statistical control strategy is demonstrated using the Lorenz '96 system and a turbulent barotropic system with topography and a large number of instabilities.

Keywords: statistical control, statistical energy principle, linear response theory

1. Background and Introduction

Control of complex turbulent flows is a general problem that occurs in many areas of science and technology, for example, in mitigating the effects of climate change and the design of technology in aerodynamic drag reduction [1, 2, 3]. The problem can be simply stated as: given the initial configuration of the states at time t_0, how to characterize and construct the optimal course of action (control) for driving the dynamical system of interest to approach a desired final condition so that a minimum cost function (control cost) can be achieved up to some specific future time $T > t_0$. The cost function usually consists of a combination of the running time payoff along the controlled trajectory in time interval (t_0, T), and the terminal state cost at the final control time T constraining the error in the final state. Solving the control problem in complex turbulent dynamical systems is always challenged by difficulties of large instabilities and strong nonlinear exchange of energy in different scales [3, 4, 5].

Dynamic programing offers an important approach to the design of optimal controls by solving a nonlinear PDE system, i.e. the Hamilton-Jacobi-Bellman (HJB) equations [6, 7]. Given a quadratic cost function in the control input, the HJB equations can be reduced to a particular PDE system [8, 7]. In solving this HJB PDE directly using various numerical solvers, the curse of dimensionality appears as one of the major obstacles when the system becomes genuinely high dimensional [9, 5]. Control of the linearized flow field near a basic mean state is an important and well-developed discipline, such as the progress in adaptive control and stabilization of fluid turbulence [3, 10]. On the other hand, methods for controlling perturbed responses in highly turbulent systems remain a challenging problem due

*Corresponding author
Email addresses: jonjon@cims.nyu.edu (Andrew J. Majda), qidi@cims.nyu.edu (Di Qi)

to the inherent nonlinearity, high-dimensionality, and time mixing [11, 12, 13]. Most model-based control designs for nonlinear system are based on the linearization of the evolution equation, then the stabilization of the unstable fixed point or periodic orbit becomes the central problem [4, 10, 14]. The high dimensional phase space and large number of instabilities of the turbulent systems require new effective and efficient control strategies.

In this paper, we discuss an alternative statistical control strategy for inhomogeneous turbulent dynamical systems. The major goal is to develop an effective control method to drive perturbed statistical solutions of complex turbulent dynamical system back to the small neighborhood of the original unperturbed target statistical equilibrium state. We begin with the general setup of turbulent dynamical systems with energy conserving nonlinearity. Instead of deriving the HJB PDE of the original system in a high dimensional phase space, the HJB equation is first developed based on a statistical energy principle where a statistical scalar identity combining the energy in the mean and the total variance becomes the central object to control. Instability will not appear in this statistical energy equation due to the symmetry in the nonlinear interactions [15, 16]. Thus the major difficulty in stabilizing many directions of instability in controlling the original equation is circumvented. The general control strategy is proposed combining the total statistical energy principle and the linear response theory based on the framework first developed in [17]. The *attractive features* in this statistical control method include that: i) only the initial total statistical change in the mean and variance is required for the statistical control regardless of the formal history of the complex system; ii) a simple scaler equation for total statistical energy in mean and variance is used to monitor the overall changes in model statistics so that the control of large dimension of instability need not be considered in any detail; iii) simple autocorrelation functions of the target statistical equilibrium alone are used to characterize the model sensitivity to perturbations in leading order with robust performance, so that the specific control forcing can be determined offline without the need to run the specific complex system to get the response. In addition, even though the control strategy is first developed in the regime of small perturbations within the linear response theory, the control skill is confirmed here from various test cases with even larger perturbation amplitudes.

With the help of the dynamical equation of the total statistical energy [15], instead of tracking the state variables in a high dimensional phase space we are able to focus on a scalar system with a linear control problem. The time rate of change of statistical energy has a tendency to decay subject to only the product of the statistical mean and forcing control. Then the optimal control forcing is recovered by solving a nonlocal inversion problem with linear response approximation of the mean state. The linear response operator to predict mean response is fit in a simple linear model with assumed diagonal structure, thus simple dynamics for the final control forcing can be developed. Model errors occur in the statistical control model through leading order approximations in both the statistical energy equation and the linear response prediction for the mean. In the first stage to illustrate the effectiveness of the method, we use a simple homogeneous perturbation case where only a scalar control forcing is needed. The simple homogeneous case enables us to investigate the control performance with different parameter values and different control calibrations to achieve a thorough understanding about the statistical control method. In the next stage, we move on to consider a more general case where inhomogeneous perturbations are involved. The dynamical system in this inhomogeneous perturbation case is still controlled by the same homogeneous control strategy on the uniform mean state as the previous case. Thus the same set of equations can be easily applied to the more complicated control scenario. While several levels of model errors are included in the control model, the robustness of the statistical control procedure maintains the high skill in the control performance. In the last stage, we compare some generalizations in the control of the statistical energy equation where second-order nonlinear effects are taken into account.

For the verification of the statistical control method, we apply the developed strategies first to the Lorenz '96 system (L-96) [18] with both homogeneous and inhomogeneous perturbations. The L-96 model is a 40-dimensional prototype model which can generate a wide variety of distinct statistical features from highly non-Gaussian to near-Gaussian regimes [19], making it a desirable model to test the control performance under various perturbation scenarios. Then the same framework is applied to geophysical turbulence [12], so that the control procedure is generalized to the barotropic model with topography. This simple model creates a large-scale mean flow with shifting directions interacting with the vortical modes through topographic stress, and inhomogeneous equilibrium mean state and forcing due to the topography need to be treated [20]. These two representative test models display many typical features of nonlinear non-Gaussian structures with a large number of instabilities that are common in the natural systems that need to be controlled [16].

The structure of the paper is as follows. In Section 2, a general formulation of the statistical control problem is stated with a description of the nonlinear dynamical system with energy conservation principle and the two-stage pro-

cedure of the general control strategy is introduced; then a more detailed derivation of the optimal statistical control algorithm is developed. In Section 3 the verification of this control performance is first illustrated in a homogeneous framework. The control strategy is generalized to the inhomogeneous perturbed case in Section 4 with more complicated scenarios. We end this paper with a summary and final discussion in Section 5.

2. General Formulation of the Statistical Control with Statistical Energy Functional

First we describe the general statistical control strategy for a quadratic system with conservative nonlinear dynamics. In particular, the general turbulent dynamical system can be formulated in the abstract form [16] about the state variables of interest $\mathbf{u} \in \mathbb{R}^N$ in a high dimensional phase space

$$\frac{d\mathbf{u}}{dt} = (L + D)\,\mathbf{u} + B(\mathbf{u}, \mathbf{u}) + \mathbf{F}(t) + \sum_k \sigma_k(\mathbf{u}, t)\,\dot{W}_{k,t}, \tag{2.1}$$

where $L^* = -L$ is a skew-symmetric linear operator; $D^* = D$ is a negative definite symmetric operator; and the quadratic operator $B(\mathbf{u}, \mathbf{u})$ conserves energy by itself so that $\mathbf{u} \cdot B(\mathbf{u}, \mathbf{u}) = 0$. For example in climate models, L could represent the β-effect of Earth's curvature, D could represent dissipative processes such as surface drag, radiative damping, viscosity, etc. Besides, the turbulent system is always subject to climate change forcing effects both from the large-scale deterministic part $\mathbf{F}$, and from the unresolved small-scale stochastic part $\sigma_k(\mathbf{u}, t)\,\dot{W}_{k,t}$. Especially, such systems as (2.1) contain many degrees of instabilities due to the internal nonlinear interactions $B(\mathbf{u}, \mathbf{u})$ between different scales [21, 22], thus the computational cost in directly controlling this system quickly becomes intractable as the dimensionality increases [7, 4]. It is useful to consider the statistical behavior of the state variables $\mathbf{u}$ with uncertainty, and we are mostly interested in an efficient control of the leading order statistics (such as mean $\bar{\mathbf{u}}$ and variance R) near the original statistical steady state $\left(\bar{\mathbf{u}}_{\text{eq}}, R_{\text{eq}}\right)$ for dynamical systems in the form of (2.1) due to unknown forcing perturbations based on a proper statistical energy identity [16, 15].

Importantly the turbulent dynamical systems (2.1) have a general statistical energy principle due to the symmetry in the nonlinearity, $\mathbf{u} \cdot B(\mathbf{u}, \mathbf{u}) = 0$, with many applications [16, 19, 21, 20]. For simplicity in exposition, assume that the damping operator is a constant multiple of the identity, $D = -dI, d > 0$. Under suitable general assumptions detailed in [15], the turbulent dynamical system (2.1) satisfies the total statistical energy conservation principle for the *statistical energy functional*,

$$E = \frac{1}{2}\bar{\mathbf{u}} \cdot \bar{\mathbf{u}} + \frac{1}{2}\text{tr}R, \tag{2.2}$$

that combines statistics in mean energy and total variance so that the rate of change in the total statistical energy is directly linked with the change in the first order statistical mean and forcing-dissipation structure

$$\frac{dE}{dt} = -2dE + \bar{\mathbf{u}} \cdot \mathbf{F} + \Sigma, \tag{2.3}$$

Above $\bar{\mathbf{u}} = \langle \mathbf{u} \rangle$ is the statistical mean of the state variables and $R = \langle (\mathbf{u} - \bar{\mathbf{u}}) \otimes (\mathbf{u} - \bar{\mathbf{u}}) \rangle$ is the covariance matrix; $\Sigma = \frac{1}{2}\sum_{k=1}^{N} \sigma_k^2$ is the total effect of random forcing in the system. On the right hand side of the scalar equation (2.3), besides the uniform damping the forcing is only applied on the mean state $\bar{\mathbf{u}}$. This system (2.3) is stable with statistical identity E served as a statistical Lyapunov function [16]. The advantage of using this total statistical energy equation in the control problem is that it effectively avoids the inclusion of complex nonlinear interaction effects $B(\mathbf{u}, \mathbf{u})$ including various internal instability of the turbulent system in the first stage and makes it possible to concentrate on the central dominant energy mechanism using only the statistical mean state $\bar{\mathbf{u}}$, which is easy to estimate with accuracy in practice.

In the remainder of this section, we offer an overview of the general statistical control strategy based on the total statistical energy conservation principle (2.3) and linear response theory, which is first introduced in a recent paper [17] in a simple setup. We also include the approximations and detailed formulas for the statistical control algorithm for general inhomogeneous complex turbulent systems.

2.1. Statistical control of nonlinear system with linearized statistical energy identity

The two major mathematical tools used in the construction of statistical control strategy is the statistical energy conservation principle for estimating the total statistical fluctuation in the system and linear statistical response theory for predicting leading order responses in the statistical mean state [22, 23, 24]. Applying these two mathematical tools to the original nonlinear complex systems (2.1), we derive the linearized control equation of the statistical energy fluctuation for the general control problems.

2.1.1. Linearized statistical energy equation about fluctuation

In order to monitor the evolution of perturbed statistics away from the target statistical equilibrium due to external forcing, we consider the statistical energy fluctuation by separating the statistical equilibrium state $E_{\rm eq}$

$$E'(t) = E(t) - E_{\rm eq}, \quad E_{\rm eq} = (2d)^{-1}\left(\bar{\mathbf{u}}_{\rm eq}\cdot\bar{\mathbf{F}}_{\rm eq} + \Sigma\right), \tag{2.4}$$

where the statistical equilibrium total energy $E_{\rm eq} = \frac{1}{2}\left|\bar{\mathbf{u}}_{\rm eq}\right|^2 + \frac{1}{2}{\rm tr}R_{\rm eq}$ and statistical mean state $\bar{\mathbf{u}}_{\rm eq}$ are assumed from the equilibrium invariant measure of the original unperturbed system (2.1). $\bar{\mathbf{F}}_{\rm eq}, \Sigma$ are the effects of deterministic and stochastic forcing in unperturbed equilibrium. $E_{\rm eq}$ can be directly calculated from the energy equation (2.3) where the left hand side vanishes in statistical steady state. Especially in controlling the statistical energy fluctuation E' via a deterministic forcing on the mean state, we automatically succeed in controlling the second order variance fluctuation, $\delta{\rm tr}R$, once the mean state fluctuation $\delta\bar{\mathbf{u}}$ is controlled to zero (or a small value).

In general the dynamical system is subject to various kinds of perturbations $\delta\mathbf{F}$ (and the external forcing $\delta\mathbf{F}$ could be inhomogeneous) on top of the equilibrium forcing $\bar{\mathbf{F}}_{\rm eq}$. We focus on controlling the high dimensional turbulent system through deterministic control on statistical fluctuations about the equilibrium mean state $\delta\bar{\mathbf{u}} = \bar{\mathbf{u}} - \bar{\mathbf{u}}_{\rm eq}$. By subtracting the equilibrium state solution (2.4) from the original statistical energy dynamics (2.3) we get the dynamical equation for the fluctuation component E'

$$\frac{dE'}{dt} = -2dE' + \bar{\mathbf{u}}\cdot\mathbf{F} - \left(\bar{\mathbf{u}}_{\rm eq}\cdot\bar{\mathbf{F}}_{\rm eq}\right) = -2dE' + \bar{\mathbf{u}}_{\rm eq}\cdot\delta\mathbf{F} + \bar{\mathbf{F}}_{\rm eq}\cdot\delta\bar{\mathbf{u}} + \delta\bar{\mathbf{F}}\cdot\delta\bar{\mathbf{u}}.$$

The unperturbed system may also subject to a random forcing effect Σ which will not change the fluctuation component in E'. In controlling the total fluctuation statistical energy E' we consider the equation linearized in the leading order expansion due to perturbations by assuming that the forcing and mean perturbation coupling $\delta\bar{\mathbf{F}}\cdot\delta\bar{\mathbf{u}} = O\left(\delta^2\right)$ is a higher order term. In addition, with the help of the statistical energy equation, once we have the responses in the mean perturbation, $\delta\bar{\mathbf{u}}$, the responses in the total variance $\delta R = R - R_{\rm eq}$ (and equivalently, the single-point variance at each grid point) can be recovered from the total statistical energy (2.2), $E = \frac{1}{2}|\bar{\mathbf{u}}|^2 + \frac{1}{2}{\rm tr}R$. Thus by controlling the perturbation in the first-order mean state through the statistical energy equation, we are able to control the changes in the one-point second-order variance at the same time.

In controlling the perturbed dynamics (2.1) according to the scalar statistical dynamics (2.3), introduce a truncated orthonormal basis $\{\mathbf{e}_k\}_{k=1}^N$ under suitable choice of inner product. For example, $\mathbf{e}_k$ could be the effective orthogonal functions (EOF) containing most of the energy in the equilibrium $R_{\rm eq}$ is captured. The equilibrium mean state and external forcing can be expanded by projection to the basis

$$\bar{\mathbf{u}}_{\rm eq} = \sum_k \bar{u}_{{\rm eq},k}\mathbf{e}_k, \quad \bar{\mathbf{F}}_{\rm eq} = \sum_k \bar{F}_{{\rm eq},k}\mathbf{e}_k. \tag{2.5}$$

The (deterministic) control for the statistical mean state then can be introduced as one additional vector forcing $\vec{\kappa}(t)$ through

$$\delta\mathbf{F} \equiv \vec{\kappa}(t) = \sum_{k=1}^{M}\kappa_k(t)\,\mathbf{e}_k,$$

where the control forcing $\vec{\kappa}(t)$ applies on the selected first M leading modes, which could also include the most sensitive directions of the system. In general, $\kappa_0(t)$ controls the uniform mean state $\bar{u} = \frac{1}{N}\sum_j \bar{u}_j$ in mode $\mathbf{e}_0$, and $\kappa_k(t)$ is for the response in the k-th small scale mode $\mathbf{e}_k$. Combining all these formulations, the statistical energy fluctuation

equation with leading order responses in the mean can be written with respect to the forcing perturbation along the orthonormal modes $\{\mathbf{e}_k\}_{k=1}^M$

$$\frac{dE}{dt} = -2dE(t) + \sum_{k=1}^{M}\left[\bar{u}_{\mathrm{eq},k}\cdot\kappa_k(t) + \bar{F}_{\mathrm{eq},k}\cdot\delta\bar{u}_k(t;\vec{\kappa})\right], \quad E(0) = E_0. \tag{2.6}$$

Above and later the primes for the fluctuation components are dropped in the statistical energy fluctuation E', and E_0 is the initial total statistical energy perturbation to be controlled. $\delta\bar{u}_k(t;\vec{\kappa})$ is the mean response in the k-th mode subject to the control forcing $\vec{\kappa}$. In the dynamical equation (2.6) we only use leading order responses in order $O(\delta)$ by assuming the external forcing perturbation is kept in small amplitude. Through the various numerical tests shown later in Section 3 and 4 it can be found that this approximation is actually effective for a wide range of perturbations even with larger amplitudes.

2.1.2. Linear statistical response for mean state

In the linearized statistical equation (2.6), the statistical response in the mean state, $\delta\bar{\mathbf{u}}$, is related with the explicit form of the external perturbation (or control) $\vec{\kappa}$ exerted on the system. The computational expense through direct number simulation of (2.1) to achieve the mean state will soon become unaffordable as the dimensionality of the system increases. Alternatively, linear response theory based on the fluctuation-dissipation theorem (FDT) [25, 23, 22, 24] offers a convenient way to estimate the leading order responses in statistics. Specifically, the response in the leading order mean state, $\delta\bar{\mathbf{u}}$, subject to the external forcing $\vec{\kappa}(t)$ can be estimated using the mean response operator

$$\delta\bar{u}_k(t) = \sum_{l=1}^{N}\int_0^t \mathcal{R}_{\bar{u},kl}(t-s)\,\kappa_l(s)\,ds + O\left(\delta^2\right).$$

Above $\mathcal{R}_{\bar{u},kl}(t) \equiv \mathcal{R}^l_{\bar{u}}(t)\,\mathbf{e}_k$ is called the *linear response operator* for the contribution of the l-th component of the forcing κ_l to the statistical mean state $\delta\bar{u}_k$ in k-th component, where a linear leading order approximation is valid. FDT states that the linear response operator can be calculated only requiring information from the target equilibrium statistics

$$\mathcal{R}_{\bar{u}}(t) = \langle \mathbf{u}(t)\,B[\mathbf{u}(0)]\rangle_{\mathrm{eq}}, \quad B(\mathbf{u}) = -\mathrm{div}_{\mathbf{u}}\left(\mathbf{w}p_{\mathrm{eq}}\right)/p_{\mathrm{eq}}, \tag{2.7}$$

with $\delta\mathbf{F} = \mathbf{w}(\mathbf{u})\,\delta f(t)$. In general the linear response operator is difficult to calculate considering the complicated and unaccessible equilibrium distribution, and various approximation techniques have been proposed [26, 27, 23, 22].

Especially if we make quasi-Gaussian approximation for the invariant measure of the system in (2.7), that is, set $p_{\mathrm{eq}} \propto \exp\left[-\frac{1}{2}\left(\mathbf{u}-\mathbf{u}_{\mathrm{eq}}\right)^T R_{\mathrm{eq}}^{-1}\left(\mathbf{u}-\mathbf{u}_{\mathrm{eq}}\right)\right]$ and $\mathbf{w}(\mathbf{u}) = \mathbf{e}_l$ for each perturbed direction, the linear response operator for the mean becomes a combination of time-lagged correlation functions [22, 23]

$$\mathcal{R}_{\bar{u},kl}(t) = \left\langle\left(u_k(t+s) - \bar{u}_{k,\mathrm{eq}}\right)\mathbf{e}_l\cdot R_{\mathrm{eq}}^{-1}\left(\mathbf{u}(s) - \bar{\mathbf{u}}_{\mathrm{eq}}\right)\right\rangle. \tag{2.8}$$

As shown in the quasi-Gaussian approximation (2.8), the linear response operator $\mathcal{R}_{\bar{u}}(t)$ should include various feedbacks from different scales due to nonlinear interactions between modes [26, 27]. While they can have model errors at long time response, judicious simple linear regression models [23, 28, 29] for approximating the mean statistical response are an attractive option here.

In practice if we choose EOFs as the orthonormal basis $\{\mathbf{e}_k\}$, the equilibrium covariance $R_{\mathrm{eq}} = \mathrm{diag}\left\{r_{\mathrm{eq},1},\cdots,r_{\mathrm{eq},N}\right\}$ in (2.8) is diagonalized under the EOF basis, where $r_{\mathrm{eq},k}$ is the equilibrium variance for the uncertain coefficient of mode $\mathbf{e}_k$ and cross-covariances between different mode vanish. We ignore lagged cross-correlations in this EOF basis. Then the N-by-N linear response operator $\mathcal{R}_{\bar{u}}(t)$ can also be built as a diagonal matrix with diagonal components as scalar autocorrelations in each mode

$$\mathcal{R}_{\bar{u}}(t) = \mathrm{diag}\left\{r^1_{\bar{u}}(t),\cdots,r^N_{\bar{u}}(t)\right\}, \quad N\times N \text{ diagonal response matrix}, \tag{2.9}$$

with the response operator in k-th mode $r^k_{\bar{u}}(t) = r^{-1}_{\mathrm{eq},k}\langle u_k(t)\,u_k(0)\rangle$. With the simplification in (2.9) the mean responses in mode $\mathbf{e}_k$ can be calculated just based on the autocorrelation function on the k-th mode

$$\delta\bar{u}_k(t) \equiv \mathcal{L}_{\bar{u},k}(t) = \int_0^t \mathcal{R}_{\bar{u},k}(t-s)\,\kappa_k(s)\,ds, \quad \mathcal{R}_{\bar{u},k}(t) = \langle u_k(t)\,u_k(0)\rangle/r_{\mathrm{eq},k}. \tag{2.10}$$

In this way, the linear response in each direction $\delta\bar{u}_k$ gets decoupled with each other only related with the forcing on the corresponding mode κ_k. This enables us to solve the optimal control forcing $\kappa_k(t)$ componentwise with much efficiency as we can see next. In the special case when diagonal linear Gaussian models are used to approximate the system, this above linear response operator approximation becomes exact for predicting the responses in mean state. Further we assume *no additional random noise perturbation* adding on the fluctuation equation in the first stage purely for simplicity. Similar response operators for random perturbations can also be derived in a similar way as in (2.7).

Efficient statistical control strategy from leading order statistical energy fluctuation and mean response

Using the linearization in both the statistical energy equation and the leading order mean response, the control problem of the statistical energy fluctuation becomes linear involving equilibrium statistics $\left(\bar{\mathbf{u}}_{\text{eq}}, \bar{\mathbf{F}}_{\text{eq}}\right)$ and autocorrelation functions $\mathcal{R}_{\bar{u}}(t)$ representing the memory in the state variable. The task then is to find proper formula for the ideal *optimal control forcing* $\vec{\kappa}(t)$ on the mean state to drive the perturbed energy fluctuation E back to zero (or close to zero) efficiently with minimum cost. Combining both the approximations in (2.6) and (2.10), the ***statistical control equation in leading order responses*** can be rewritten from the original statistical dynamics as

$$\frac{dE}{dt} = -2dE(t) + \sum_{k=1}^{M}\left[\bar{u}_{\text{eq},k}\cdot\kappa_k(t) + \bar{F}_{\text{eq},k}\cdot\int_0^t \mathcal{R}_{\bar{u},k}(t-s)\,\kappa_k(s)\,ds\right], \quad E(0) = E_0. \tag{2.11}$$

The control system (2.11) is linear but involves nonlinear statistical functionals as coefficient from the target unperturbed equilibrium measure. Note that the linear response operator $\mathcal{R}_k$ introduces *non-Markovian forcing* into the system through the convolution, thus the history in the forcing control $\vec{\kappa}(t)$ also matters. Linearization errors from the above system come from i) the higher-order mean-forcing interaction, $\delta\bar{u}\cdot\delta F$; and ii) the higher-order corrections for the linear response of the mean, $\delta\bar{u}$. The statistical control on the nontrivial system (2.1) through (2.11) only requires initial statistical data $E(0) = E_0$ that can be determined through observations or perfect and low-order model simulations, and the autocorrelation functions $\mathcal{R}_{\bar{u}}$ only on the most sensitive perturbed directions [22, 23].

2.2. Effective statistical control strategy in two steps

Here we derive the formulas for solving the general statistical control problem with the energy fluctuation identity $E(t)$. For controlling the statistical energy through the equation, we introduce a *local statistical control* $C(t)$ as a nonlocal functional of the scalar control forcing $\vec{\kappa}(t)$ containing all the perturbed feedbacks in the statistical energy fluctuation in (2.11). The statistical control $C(t)$ is defined from the statistical feedbacks in each controlled direction as

$$C(t) = \sum_{k=1}^{M} C_k = \sum_{k=1}^{M}\left[\bar{u}_{\text{eq},k}\cdot\kappa_k(t) + \bar{F}_{\text{eq},k}\cdot\int_0^t \mathcal{R}_{\bar{u},k}(t-s)\,\kappa_k(s)\,ds\right]. \tag{2.12}$$

In this way, we need just focus on this statistical control operator $C(t)$ for total statistical energy $E(t)$ in the first step regardless of the explicit forms of the mean state and specific forcing perturbations or exact equilibrium statistics. Therefore the *general statistical control procedure* can be decomposed into the following two consecutive steps:

i) find the optimal statistical control strategy for $C(t)$ through dynamic programming in the total statistical energy equation (2.11);

ii) invert the (nonlocal) functional $C(t)$ to get the explicit forcing control strategy for $\kappa(t)$ using the leading order mean responses in (2.12).

2.2.1. Optimal control on statistical energy identity

In the first step of constructing statistical control $C(t)$, the linear statistical control problem can be solved directly following *dynamic programming* [6, 9] by solving the Hamilton-Jacobi-Bellman (HJB) equation. In this linear scalar control problem, the statistical control $C(t)$ can be purely determined by the dissipation of the original dynamical system, and the HJB equation becomes the *Riccati* equation [8, 17]. We first construct the linear statistical control problem by proposing a proper cost function to optimize. With the statistical control $C(t) = \sum_k C_k$ defined with a

combination of the contributions from each mode $\mathbf{e}_k$ in (2.12), the control system becomes the linear scalar dynamical equation between time interval $[t, T]$

$$\frac{dE}{ds} = -2dE(s) + \sum_k C_k(s), \quad E(t) = x, \ t \le s \le T, \tag{2.13}$$

regardless of the specific structure in the functional $C(t)$. We attempt to minimize the *cost function* as a quadratic combination of the energy fluctuation E and control functional in each mode C_k

$$\mathcal{F}_\alpha[C_k(\cdot)] \equiv \int_t^T \left[E^2(s) + \sum_{k=1}^M \alpha_k C_k^2(s)\right] ds + k_T E^2(T), \tag{2.14}$$

so that the optimal control solution $C^*(t)$ is reached at the minimum value of the cost function $\min_C \mathcal{F}_\alpha[C(\cdot)]$. The cost function (2.14) is defined in the simplest form as a quadratic combination about the statistical energy $E(t)$ and the statistical control $C(t)$. The weighting parameter $\alpha_k > 0$ is introduced to add a balancing factor between the control efficiency (due to E) and the control expense (due to C_k). Larger value of α_k adds more constraint on the control component so weaker control is introduced to the direction $\mathbf{e}_k$. Besides, the additional parameter k_T sets the importance weight of the end value of the total energy $E(T)$. It calibrates how large error is concerned at the final controlled state of the energy fluctuation. It is useful when we want fast restoration in a short control time.

We derive the optimal control solution $C^*(t)$ for control time window $[0, T]$ with cost functions $\mathcal{F}_\alpha$ in (2.14) depending on parameter values $\{\alpha_k, k_T\}$. It is known that the control problem with a quadratic cost function in the linear system (2.13) can be solved by the HJB equation through dynamic programing [8, 7]. The optimal value function then can be introduced as the minimized cost function

$$v(x,t) = \min_C \mathcal{F}_\alpha[C(\cdot)], \quad v(x,T) = k_T E^2(T).$$

In the above optimal value function $v(x,t)$, t is the initial time when the control starts, and x is the initial perturbation in the total statistical energy $x = E(t)$. The final time T can be determined as the time when the final fluctuation energy is small enough, $E(T) \ll 1$. Assuming the value function $v \in C^1$, the value function $v(x,t)$ satisfies the HJB equation

$$\begin{aligned} v_t(x,t) + \max_{c_1,\cdots,c_k} \sum_k \left(\alpha_k c_k^2 + v_x c_k\right) + \left(x^2 - 2dxv_x\right) = 0, \quad 0 \le t < T, \\ v(x,T) = k_T x^2. \end{aligned} \tag{2.15}$$

The form of the solution $v(x,t)$ can be guessed also in a quadratic form due to the linear dynamics (2.13) and the quadratic cost function, so suppose

$$v(x,t) \equiv K(t)\, x^2.$$

After simple calculation by substituting the quadratic form of $v(x,t)$ back into (2.15), the solution of the above HJB equation can be found by solving a Riccati equation for $K(t)$, that is,

$$\begin{aligned} \frac{dK}{dt} &= \sum_k \alpha_k^{-1} K^2 + 4dK - 1, \quad 0 \le t < T, \\ K(T) &= k_T. \end{aligned} \tag{2.16}$$

This is a backward equation in time about $K(t)$. With the solution of the Riccati equation $K(t)$, the optimal feedback control $C_k^*(t)$ together with the optimal control statistical equation for E^* can be found by the maximum value from the second term of (2.15)

$$\begin{aligned} C_k^*(t) &= -\alpha_k^{-1} K(t) E^*(t), \quad k = 1, \cdots, M, \\ \frac{dE^*}{dt} &= -\left[2d + \sum_k \alpha_k^{-1} K(t)\right] E^*(t), \end{aligned} \tag{2.17}$$

with the initial condition of fluctuation energy $E^*(0) = E_0$. Above $-\alpha_k^{-1} K(t) E^*(t)$ defines the feedback control due to the minimum cost constraint. It works as one additional damping effect that drives the total statistical energy fluctuation $E(t)$ back to zero in an efficient way.

As a final comment, in the cost function $\mathcal{F}_\alpha$ different parameters α_k are introduced for each controlled direction $\mathbf{e}_k$. Usually the more energetic modes become more sensitive to external perturbations according longer mixing time in the autocorrelations and linear response, thus smaller penalty is added in the more energetic directions in the cost function $\mathcal{F}_\alpha$. Therefore we may propose a further simplification for the general control weights so that,

$$\alpha_k = \alpha w_k^{-1}, \quad w_k = \frac{r_{\mathrm{eq},k}}{\sum_k r_{\mathrm{eq},k}}. \tag{2.18}$$

where $\alpha > 0$ becomes the single weighting parameter to be determined and the difference between the controlled modes are determined from the equilibrium variance r_{eq}. In this way, more energetic modes will be assigned with stronger control so that balanced control is introduced along each direction. As we will see in Section 4, this choice of model parameters makes the general control Riccati equation for K and energy equation E (2.16) and (2.17) stay exactly the same form as the special homogeneous case in (3.3) and (3.2). It will offer convenience for the numerical implementations in a consistent framework. We will show more of the solution features in the optimal statistical solution with examples in Section 3.1. Of course, if (economic) cost considerations matter the general form can be easily adopted below.

2.2.2. Attribution of the optimal statistical control

Next assume that we have solved the optimal statistical control $C_k(t)$ in each direction $\mathbf{e}_k$ through controlling the general statistical energy identity. The second step of the problem is about finding the optimal control forcing $\kappa_k(t)$ to apply on the corresponding perturbed mode $\mathbf{e}_k$ through the nonlinear inversion about the implicit relation in (2.12). In fact, we can always consider each component C_k in (2.12) separately in this step of statistical control attribution since each C_k has been recovered in (2.17) in the explicit formula, and the linear response in mean is decoupled with forcing perturbation κ_k in each direction thanks to the diagonalized autocorrelations in (2.9). Then the final solution $\vec{\kappa}(t) = \sum_k \kappa_k \mathbf{e}_k$ can be combined with all the control feedbacks that are solved individually. In addition, the coefficients by projection to mode $\mathbf{e}_k$ could take complex values depending on the choice of a complex valued orthonormal basis (for example, the Fourier basis in periodic boundary condition). Therefore the attribution of the optimal statistical control becomes the non-Markovian inversion problem in each of the controlled directions $\mathbf{e}_k$ due to convolution with the linear response factor $\mathcal{R}_{\bar{u}}$ including memories

$$C(t) = \bar{u}_{\mathrm{eq}} \kappa^*(t) + \bar{F}^*_{\mathrm{eq}} \mathcal{L}_{\bar{u}}(t) \equiv \bar{u}_{\mathrm{eq}} \kappa^*(t) + \bar{F}^*_{\mathrm{eq}} \int_0^t \mathcal{R}_{\bar{u}}(t-s)\, \kappa(s)\, ds, \tag{2.19}$$

where the inner-product in (2.12) needs to include complex conjugate of the coefficients all decomposed into real and imaginary parts for a general complex case

$$\bar{u}_{\mathrm{eq}} = \bar{u}^r + i\bar{u}^i, \quad \bar{F}_{\mathrm{eq}} = \bar{F}^r + i\bar{F}^i, \quad \kappa(t) = \kappa^r(t) + i\kappa^i(t).$$

Here and below in this subsection we neglect the subscript k for the statistical control in each mode $\mathbf{e}_k$ for simplicity. In an alternative way in representing the complex inner-product in (2.19), we can write the real and imaginary part separately therefore the control relation can be rewritten as as a 2×2 system with matrix coefficients (U, Γ) from the equilibrium statistics, that is,

$$C(t) = \begin{bmatrix} C^r \\ C^i \end{bmatrix} = U\mathcal{K}(t) + \Gamma \mathcal{L}_{\bar{u}}(t; \mathcal{K}), \quad \mathcal{K}(t) = \begin{bmatrix} \kappa^r \\ \kappa^i \end{bmatrix}, \; U = \begin{bmatrix} \bar{u}^r & \bar{u}^i \\ \bar{u}^i & -\bar{u}^r \end{bmatrix}, \; \Gamma = \begin{bmatrix} \bar{F}^r & \bar{F}^i \\ -\bar{F}^i & \bar{F}^r \end{bmatrix}. \tag{2.20}$$

Besides $\mathcal{L}_{\bar{u}}(t; \mathcal{K}) = \left(\delta\bar{u}^r, \delta\bar{u}^i\right)^T$ is the linear response in the mean state that in general couples the control in real and imaginary component $\mathcal{K} = \left(\kappa^r, \kappa^i\right)^T$.

The optimal statistical control $C^*(t)$ as a functional of the optimal controlled energy $E^*(t)$ by statistical control of the energy equation can be solved explicitly through the dynamical equation (2.17)

$$C^*(t) = -\alpha^{-1} K(t) E^*(t), \quad E^*(t) = \exp\left(-2dt - \tilde{\alpha}^{-1} \int_0^t K(s)\, ds\right) E_0,$$

with $\tilde{\alpha}^{-1} \equiv \sum_k \alpha_k^{-1}$. The time differentiation of $C^*(t)$ can be expressed using the dynamics of the Riccati equation (3.3) and proper rearrangement of the equations

$$\frac{dC^*}{dt} = -\alpha^{-1}\dot{K}E^* - \alpha^{-1}K(t)E^*(t)\left(-2d - \tilde{\alpha}^{-1}K(t)\right) = \left(2d - K^{-1}(t)\right)C^*.$$

Above the first equality uses the explicit solution of $E^*(t)$ and the second equality is through the Riccati equation (3.3). On the other hand, to find the dynamics to solve $\kappa(t)$, by taking time derivative of the control relation from definition (2.20) we get the dynamics that relates the statistical control $\dot{C}$ and the final control forcing $\dot{\mathcal{K}}$

$$\frac{dC}{dt} = U\frac{d\mathcal{K}}{dt} + \Gamma\frac{d\mathcal{L}_{\bar{u}}}{dt} = U\dot{\mathcal{K}}(t) + \Gamma\mathcal{K}(t) + \Gamma\int_0^t \mathcal{R}'_{\bar{u}}(t-s)\mathcal{K}(s)\,ds.$$

Above the time derivative of the autocorrelation function $\mathcal{R}'_{\bar{u}}$ is also included.

Combining the above two relations for the time derivatives about the optimal statistical control $C^*(t)$, the control forcing solution should follow the dynamical equation for real and imaginary component

$$\begin{aligned} &\left(2d - K^{-1}(t)\right)C = \dot{C} = U\dot{\mathcal{K}} + \Gamma\mathcal{K}(t) + \Gamma\int_0^t \mathcal{R}'_{\bar{u}}(t-s)\mathcal{K}(s)\,ds \\ \Rightarrow\ &\frac{d\mathcal{K}}{dt} + U^{-1}\Gamma\left(\mathcal{K}(t) + \int_0^t \mathcal{R}'_{\bar{u}}(t-s)\mathcal{K}(s)\,ds\right) - U^{-1}\left(2d - K^{-1}(t)\right)C = 0, \end{aligned} \tag{2.21}$$

where $\mathcal{K} = \left(\kappa^r, \kappa^i\right)^T$ is a 2-vector. Notice that if we set the imaginary component in the above equation (2.21) to be zero, $C^i = 0, \bar{u}^i = 0, \bar{F}^i = 0$, the matrix representation (2.20) is still valid by restricting to real values with the scalar dynamics for real part only recovered

$$\frac{d\kappa}{dt} + \bar{F}_{\mathrm{eq}}/\bar{u}_{\mathrm{eq}}\left(\kappa(t) + \int_0^t \mathcal{R}'_{\bar{u}}(t-s)\kappa(s)\,ds\right) = \left(2d - K^{-1}(t)\right)C(t)/\bar{u}_{\mathrm{eq}}.$$

Still one additional difficulty is that the derivative of autocorrelation $\mathcal{R}'_{\bar{u}}$ is usually unaccessible. Thus it required to find some proper approximation for the autocorrelation function $\mathcal{R}_{\bar{u}}$ so that the essential structures can be captured.

Linear regression fitting of the autocorrelation function. In solving the dynamical equation for $\mathcal{K}(t)$ (2.21), the key point is to propose proper form of the linear response operator $\mathcal{R}_{\bar{u}}$. We consider simple low-order in time linear regression models [23, 28, 29] to approximate the autocorrelation function $\mathcal{R}_{\bar{u}}$ in (2.10). In this way, the responses due to the forcing in each direction $\mathbf{e}_k$ get decoupled with each other. The autocorrelation simply becomes an exponential function using a linear regression model to approximate the autocorrelation $\mathcal{R}_{\bar{u}}(t)$ in each perturbed direction,

$$\mathcal{R}^M_{\bar{u}}(t) = \exp(-\gamma_M t) = \exp\left[-(d_M + i\omega_M)t\right]. \tag{2.22}$$

The imaginary parameter ω_M is used to approximate the oscillatary structure that is common in autocorrelations. In consistent with the matrix formulation (2.20) the mean response with the first-order linear response prediction (2.22) can be also written in the 2×2 matrix form

$$\mathcal{L}_{\bar{u}}(t) \equiv \begin{bmatrix}\delta\bar{u}^r \\ \delta\bar{u}^i\end{bmatrix} = \int_0^t \mathcal{R}^M_{\bar{u}}(t-s)\mathcal{K}(s)\,ds, \quad \mathcal{R}^M_{\bar{u}}(t) = e^{-d_M t}\begin{bmatrix}\cos\omega_M t & \sin\omega_M t \\ -\sin\omega_M t & \cos\omega_M t\end{bmatrix}.$$

It can be seen from the test cases in Section 3, even with real equilibrium mean and forcing $\left(\bar{u}_{\mathrm{eq}}, \bar{F}_{\mathrm{eq}}\right)$ in the control relation (2.19) it is still useful to consider complex values in $\mathcal{R}_{\bar{u}}$ for better fitting in the autocorrelations. (2.22) is equivalent to using an independent Gaussian linear dynamical model for each coefficient u_k of mode $\mathbf{e}_k$ from an Ornstein-Uhlenbeck process, $du_k = -\gamma_M u_k dt + \sigma_M dW$. The model parameter σ_M could be estimated from the equilibrium variance in the corresponding mode e_k, $\sigma_k^2 = r_{\mathrm{eq},k}/2d_M$; and the optimal parameter value for $\gamma_M = -d_M + i\omega_M$ is chosen by a spectral information criterion compared with the true data. The information-theoretic framework summarized in Appendix B [28, 29] is used which offers an efficient way to reach the optimal model

parameters with high accuracy. We offer some more details about the strategy in finding the optimal model parameters in Appendix B, and the fitting results will be discussed with examples in Section 3 and 4.

Therefore with the linear model approximation the derivative of autocorrelation function $\mathcal{R}_{\bar{u}}^{M}$ becomes easy to calculate with model parameter d_M, ω_M through direct calculation in the matrix

$$\mathcal{R}_{\bar{u}}^{M\prime} = -d_M \mathcal{R}_{\bar{u}}^{M}(t) - \omega_M e^{-d_M t}\begin{bmatrix}\sin\omega_M t & -\cos\omega_M t\\ \cos\omega_M t & \sin\omega_M t\end{bmatrix}.$$

The corresponding linear response for the mean state $\mathcal{L}_{\bar{u}} = \mathcal{R}_{\bar{u}} * \mathcal{K}$ is then used to approximate the first-order prediction in the mean $\delta\bar{u}$ with the autocorrelation function approximation. By simple arrangement the differentiation of the linear response operator in $\mathcal{R}_{\bar{u}}^{M}$can still be expressed as the interaction with a linear operator

$$\Gamma\int_0^t \mathcal{R}_{\bar{u}}^{M\prime}(t-s)\mathcal{K}(s) = \Gamma_1\mathcal{L}_{\bar{u}} = \Gamma_1\Gamma^{-1}(C - U\mathcal{K}),$$

where the relation $\mathcal{L}_{\bar{u}} = \Gamma^{-1}(C - U\kappa)$ from the definition is again used and the new operator Γ_1 due to derivative related with the linear approximation parameter (d_M, ω_M) is defined as

$$\Gamma_1 = \begin{bmatrix}-d_M\bar{F}^r - \omega_M\bar{F}^i & -d_M\bar{F}^i + \omega_M\bar{F}^r\\ d_M\bar{F}^i - \omega_M\bar{F}^r & -d_M\bar{F}^r - \omega_M\bar{F}^i\end{bmatrix}. \tag{2.23}$$

Substituting the above approximation to the original dynamics (2.21) and using the relations in solutions (2.17), the control forcing $\kappa(t)$ in each perturbed direction can be solved from the following equation

$$\frac{d\mathcal{K}}{dt} + U^{-1}\left(\Gamma - \Gamma_1\Gamma^{-1}U\right)\mathcal{K} + U^{-1}\left[\Gamma_1\Gamma^{-1} + \left(K^{-1} - 2d\right)I\right]C = 0. \tag{2.24}$$

The initial value of $\mathcal{K}(0) = U^{-1}(C^*(0) - \Gamma\delta U(0))$ is determined from the optimal solution C^* and the observed initial mean state perturbation $\delta U = \left(\delta\bar{u}^r, \delta\bar{u}^i\right)^T$. The coefficient matrices are defined from the equilibrium functionals defined in (2.20) and (2.23). By definition the nontrivial equilibrium mean states, $\left|\bar{u}_{\mathrm{eq}}\right| \neq 0, \left|\bar{F}_{\mathrm{eq}}\right| \neq 0$, guarantee the existence of the inverse matrix U^{-1}, Γ^{-1}. The equation (2.24) is more practical in solving the solutions through numerical schemes, especially when we need an imaginary coefficient ω_M to capture the oscillating features in the autocorrelations. Actually once we get the smooth solutions for $C^*(t), E^*(t)$, the above equation (2.24) is just a first-order ODE with constant coefficient. The only information required in this step for recovering the control forcing is the autocorrelation function in the zero mode. Thus it can be solved efficiently. Again if we contraint on only real values with zero imaginary part the above system simplifies to the scalar equation

$$\frac{d\kappa}{dt} + \left(d_M + {}^{\bar{F}_{\mathrm{eq}}}\!/_{\bar{u}_{\mathrm{eq}}}\right)\kappa(t) + {}^{(d_M+2d)K(t)-1}\!/_{\alpha\bar{u}_{\mathrm{eq}}}E^*(t) = 0.$$

By solving $\kappa(t)$, we find the proposed control to force the perturbed system back to the neighborhood of initial unperturbed climate.

In summary, the important advantage in the above two-step construction of the statistical control strategy using the statistical energy equation from (2.13) and (2.19) is that, the only information required *a priori* for controlling the high-dimensional turbulent system is the initial total statistical energy perturbation E_0 and a suitable approximate linear response operator $\mathcal{R}_{\bar{u}}$ for the mean of the target statistical solution with a few autocorrelations, without running the detailed model for the complex turbulent system. In the next section, we will show that we can approximate $\mathcal{R}_{\bar{u}}$ with judicious error using the autocorrelation functions in the most sensitive directions [22, 23]. Therefore the entire control strategy can be carried out easily despite the highly complicated original turbulent dynamical system in a large phase space with instability.

3. Linear First-Order Statistical Control with Homogeneous Perturbation

In this section, we display explicitly with examples the control methods in the two steps following the general framework discussed in Section 2. The general statistical control strategy is first tested on a simple homogeneous

perturbation case. This simple setup enables us to check the control dependence on different choices of parameter values and the control performances on various statistical regimes. Furthermore this simple control framework with control on the mean state can be applied on the more generalized inhomogeneous perturbation case that will be discussed in the next section. Specifically if the *homogeneous statistics* is assumed with a scalar forcing exerted on the zero base mode $\mathbf{e}_0 = [1, \cdots, 1]^T$, the mean state becomes a scalar field and the covariance matrix becomes diagonal for the entire time [19, 22],

$$\bar{\mathbf{u}}(t) = \bar{u}(t)\,\mathbf{e}_0, \quad R(t) = \mathrm{diag}\{r_1(t), \cdots, r_N(t)\}, \quad \mathbf{F}(t) = F(t)\,\mathbf{e}_0. \tag{3.1}$$

This homogeneous system will serve as a simple prototype test case in the first place for the control strategy. As we can find from the numerical simulations later, even in the inhomogeneous perturbation case with small-scale responses, this homogeneous control forcing $\kappa(t)$ directly on the uniform mean state is very effective for controlling the entire responses in an overall sense.

3.1. Optimal statistical control from scalar Riccati equation

In the homogeneous perturbations case, (3.1) shows that the response in the mean state becomes only a scalar $\bar{u}$. Therefore we only need to consider a homogeneous control on the base mode, $\vec{\kappa}(t) = \kappa(t)\,\mathbf{e}_0$. Accordingly the original statistical control functional C (2.12) and the cost function $\mathcal{F}_\alpha$ (2.14) reduce to the simple form with only one component for the homogenous controlled mean state,

$$C(t) = \bar{u}_{\mathrm{eq}} \cdot \kappa(t) + \bar{F}_{\mathrm{eq}} \cdot \delta\bar{u}(t), \quad \mathcal{F}_\alpha \equiv \int_t^T \left[E^2(s) + \alpha C^2(s)\right] ds + k_T E^2(T),$$

where $\alpha > 0$ is the single parameter for the control weight. With the above simplifications for homogeneous statistics the optimal statistical energy dynamics of $E^*(t)$ with the optimal control $C^*(t)$ in (2.17) gets simplified as

$$\begin{aligned} C^*(t) &= -\alpha^{-1} K(t)\, E^*(t), \quad 0 \le t < T, \\ \frac{dE^*}{dt} &= -\left[2d + \alpha^{-1} K(t)\right] E^*(t), \end{aligned} \tag{3.2}$$

together with the scalar Riccati equation for $K(t)$ in (2.16)

$$\frac{dK}{dt} = \alpha^{-1} K^2 + 4dK - 1, \quad K(T) = k_T. \tag{3.3}$$

Only parameters α, k_T are required here for controlling the homogeneous state. Especially notice that if we use the weighting parameters proposed in (2.18) according to the equilibrium statistics, the same set of equations will be developed in that general case. Therefore the general framework discussed in Section 2 can also be solved in a uniform framework with (3.2) and (3.3).

The advantage of the Riccati equation (3.3) is that we can in fact derive the exact solution $K(t)$. First suppose we have the Riccati equation solution $K(t)$ by solving (3.3), then the exact solution of (3.2) can be calculated directly, that is,

$$E^*(t) = E_0 \exp\left(-2dt - \alpha^{-1} \int_0^t K(s)\, ds\right). \tag{3.4}$$

Note that $E(t)$ is actually the energy fluctuation away from the equilibrium state E_{eq}, thus it can take either positive or negative value depending on its initial state fluctuation E_0. Furthermore notice that the above optimal solution has one additional degree of freedom about the final endpoint value k_T. In practice we can always set $k_T = 1$ with a simple assumption that the the error in E^* decays fast enough. Then we can find the solution of $K(t)$ by integrating the above Riccati equation (3.3) explicitly as

$$\left|\frac{K(t) - K_-}{K(t) - K_+}\right| = C(k_T) \exp\left[2\left(4d^2 + \alpha^{-1}\right)^{1/2} (T - t)\right], \tag{3.5}$$

where $K_\pm = -2\alpha d \pm \left(4\alpha^2 d^2 + \alpha\right)^{1/2}$ are the two roots (fixed points) of the quadratic polynomial $P_2(K) = \alpha^{-1}K^2 + 4dK - 1$ on right hand side of (3.3); and $C(k_T) = \left|\frac{k_T - K_-}{k_T - K_+}\right|$ is the coefficient due to the endpoint condition. We have the

non-negative constraint for $K(t) \geq 0$ always guaranteed through the explicit solution in (3.5). It can also be observed from the explicit solution that $K(t)$ will converge backwardly in time to the stable fixed point K_+ in an exponential rate, $-\left(4d^2 + \alpha^{-1}\right)^{1/2}$, thus the steady state solution $K \equiv K_+$ is stable backwardly in time.

Special fixed-in-time solution in the limit of control parameter α

As a simple example to illustrate the performance of the controlled statistical energy, the simplest strategy is to use the fixed point value K_+ as the steady state solution. Thus the optimal solution in (3.4) becomes the simpler form

$$E^*(t) = \exp\left[-\left(4d^2 + \alpha^{-1}\right)^{1/2} t\right] E_0. \tag{3.6}$$

The parameter α is introduced to add proper amount of 'control' into the total statistical energy of the perturbed system. It is interesting to observe the solutions in the asymptotic limit of the parameter α

- low cost limit as $\alpha \to 0$: then $E \sim \exp\left(-\alpha^{-1/2} t\right) E_0$, energy decays in rate $1/\sqrt{\alpha}$ to achieve fast statistical energy decay;
- high cost regime as $\alpha^{-1} \to 0$: then $E \sim \exp\left(-2dt - (4d\alpha)^{-1} t\right) E_0$, no control is added in the leading order.

From the asymptotic behavior in (3.6), large weight on the control factor $\alpha \gg 1$ is equivalent to the case with no control added at all; while small values of $\alpha \ll 1$ means stronger forcing from the control C but increasing the cost in the total control $\int_0^T C^2(s)\, ds$ at the same time.

3.1.1. Numerical solutions of scalar Riccati equation

For a clearer illustration of the control effect on total statistical energy, it is useful to check the solutions of the Riccati equation (3.5) and the optimal statistical energy (3.4) through numerical computations. The exact solutions from (3.5) with varying parameter values are shown in Figure 3.1 with various values of α, k_T. First in the solutions of the Riccati equation for $K(t)$, all the solutions approach the stable fixed point value K_+ as time goes backwardly, and all begin with the end-point value $K(T) = k_T = 1$. The convergence rate changes according to the parameter value of α. The convergence rate goes to the slowest limit as the homogeneous damping rate $\exp(-2dt)$ when the weighting parameter increases $\alpha \to \infty$. To another limit as $\alpha \to 0$ the solution converges to the fixed point solution $K(t) = K_+$ in a rapid rate $\exp\left(-\alpha^{-1/2} t\right)$. The solutions of the optimal total statistical energy $E^*(t)$ and the optimal statistical control $C^*(t)$ both perform as an exponential decay to zero (which means that the system is driven back to equilibrium and then no further control is needed). Accordingly, larger values of α lead to slower convergence in the controlled total energy, while smaller values of α drive the energy to zero rapidly with a larger control functional cost during the initial control time.

On the other hand, it is also useful to consider the control dependence on the end-point value weight k_T when the parameter α is large and the control time window $[0, T]$ is small, which means that the control is restricted in small values in the process and strong control is required near the end time. This case is useful when the control can only be applied at limited period of time with the control strength within a limited amplitude. In the second column of Figure 3.1, we consider the case with $\alpha = 1$ and the control is restricted in time before $t < 2$. As a result, large deviations of $K(t)$ away from the fixed point K_+ is required at the end time $t = T$. The corresponding statistical energy $E^*(t)$ and optimal statistical control $C^*(t)$ then converge faster with a larger value of parameter k_T. To achieve smaller end point convergence with a short time window in T, we need to keep k_T as large as possible, but it may add too large weight on the end point cost in (2.14).

In Figure 3.2, we compare the values in each component of the minimized cost function $\mathcal{F}_\alpha$ in (2.14) as the parameter values α, k_T vary. In the limit $\alpha \to 0$ the control cost $\int_0^T C^2(t)\, dt$ in the cost becomes huge; while the cost in the total statistical energy $\int_0^T E^2(t)\, dt$ increases as $\alpha \to \infty$. With smaller values of α, the end time energy $E(T)$ can be effectively reduced due to the strong control. Thus the end-point parameter k_T to control final energy level $E(T)$ does not matter too much. On the other hand, as the values of α increases, the controlled total statistical energy decays in a slower rate thus the parameter k_T gets a more important role to make sure convergence of $E(T)$ in final time, especially when the control window $[0, T]$ is restricted in shorter time. Considering the case with short control regime up to time $T = 2$ with the parameter $\alpha = 1$, by increasing the value of k_T, the final energy $E(T)$ can be effectively

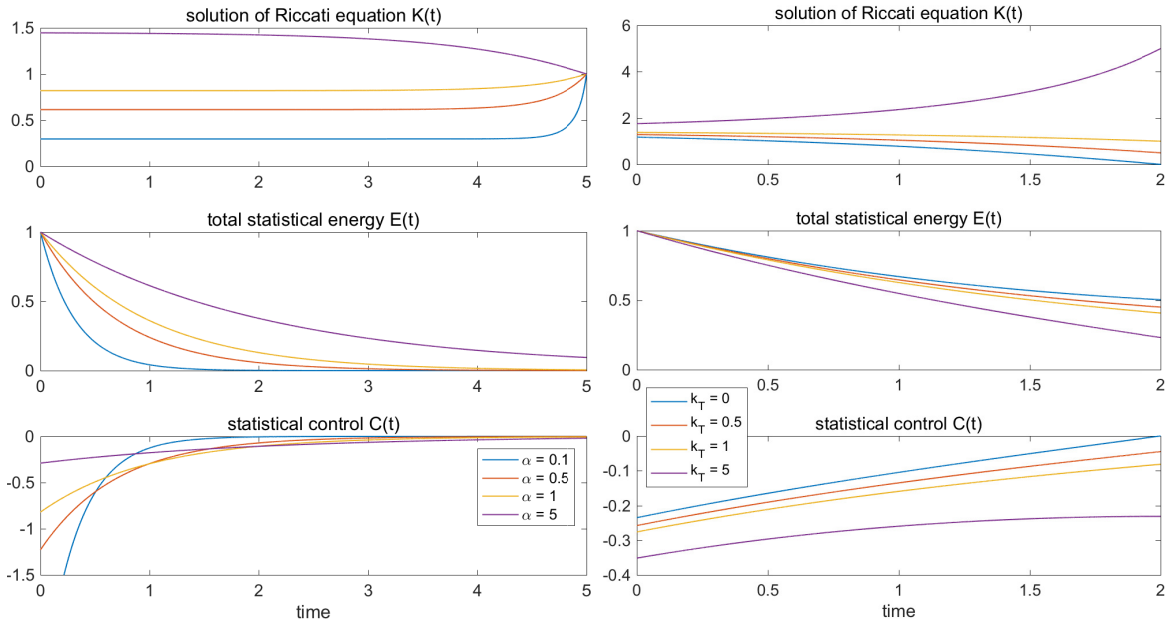

(a) solutions with different values of α, $k_T = 1$

(b) solutions with different values of k_T, $\alpha = 1$

Figure 3.1: Solutions of the Riccati equation $K(t)$, total statistical energy $E^*(t)$ under optimal control, and the optimal statistical control $C^*(t)$ with different parameter values of α and k_T.

reduced. Correspondingly the cost in the control part increases with a considerable amount, while the cost in total statistical energy decreases only in a small amount. Thus the total cost function saturated rapidly as the parameter k_T increases. The test shows that it is reasonable to just keep k_T in a relatively small value. In the following numerical experiments we will always use $k_T = 1$ in the computations if not specifically mentioned.

3.2. Numerical verification of the statistical control method using homogeneous L-96 model

Now we illustrate the control performance in the first place under the homogeneous 40-dimensional L-96 system [18] with state variables u_j such that

$$\frac{du_j}{dt} = \left(u_{j+1} - u_{j-2}\right)u_{j-1} - u_j + \bar{F}_{\text{eq}} + \delta F_0(t), \quad j = 1, \cdots, J = 40, \tag{3.7}$$

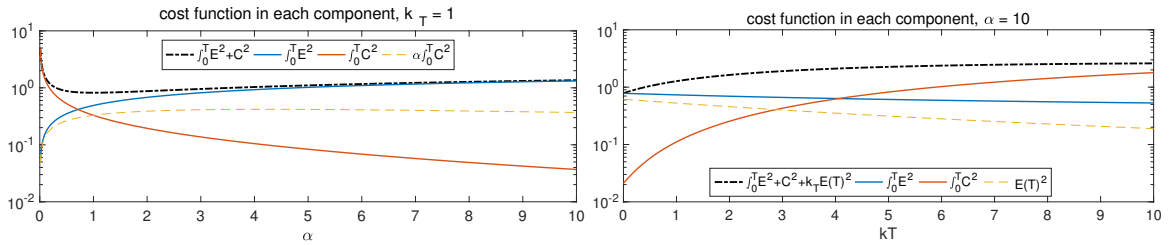

(a) costs in varying α

(b) costs in varying k_T

Figure 3.2: Comparison of the cost function $\mathcal{F}_\alpha$ in each component as the parameter values α, k_T vary under the optimal statistical control. In the first panel with changing values of α, we use the end-point parameter $k_T = 1$; while in the second panel with changing k_T, we use the slow decay case $\alpha = 1$ with short control window $T = 2$.

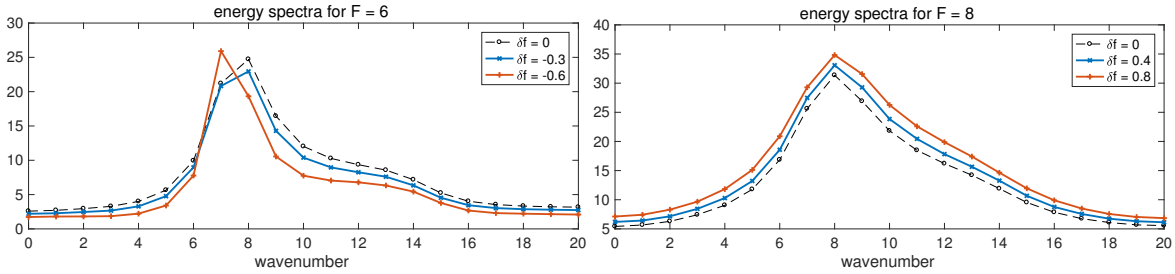

(a) $\bar{F}_{\text{eq}} = 6$ (b) $\bar{F}_{\text{eq}} = 8$

Figure 3.3: Energy spectra without and with perturbations in the two test cases $\bar{F}_{\text{eq}} = 6, 8$ in the L-96 system. The unperturbed equilibrium statistics (black lines with circle) are compared with two different amplitudes of perturbations $\delta F_0 = \pm 0.05\bar{F}_{\text{eq}}, \pm 0.1\bar{F}_{\text{eq}}$.

where both $\bar{F}_{\text{eq}}$ and δF_0 are uniform at each grid point j. The L-96 system is designed to mimic geophysical turbulence in the midlatitude atmosphere, with the energy-conserving nonlinearity in the first term on the right hand side of (3.7). Two equilibrium forcing values are taken $\bar{F}_{\text{eq}} = 6, 8$ where the system is changing from strongly non-Gaussian statistics ($\bar{F}_{\text{eq}} = 6$) to a near Gaussian regime ($\bar{F}_{\text{eq}} = 8$) with full turbulence. Stability analysis of the L-96 system shows that there exist 16 unstable modes for $\bar{F}_{\text{eq}} = 6$ case and 18 unstable modes for $\bar{F}_{\text{eq}} = 8$ case in the linearized operator around the homogeneous mean state $\bar{u}_{\text{eq}}$ [22, 19]. Thus direct control of the L-96 system requires a large number of controlled modes.

By testing the control strategy due to perturbations at different strength, we apply the external forcing δF_0 with gradually increasing amplitude. The homogeneous forcing perturbation is chosen as a ramp-type forcing

$$\delta F_0(t) = \delta f_0 \frac{\tanh a(t - t_c) + \tanh at_c}{1 + \tanh at_c},$$

increasing from 0 to the maximum δf_0, with upward forcing for $\bar{F}_{\text{eq}} = 8$, and downward forcing for $F = 6$ with a 10% ramp amplitude as $\delta f_0 = 0.1\bar{F}_{\text{eq}}$. Thus the responses due to various perturbation amplitudes can be generated. The energy (variance) spectra at each spectral mode in the two test cases are plotted in Figure 3.3. The unperturbed equilibrium spectra are compared with the perturbed cases with different perturbation amplitudes $\delta F_0 = \pm 0.05\bar{F}_{\text{eq}}$ and $\delta F_0 = \pm 0.1\bar{F}_{\text{eq}}$. Especially in the weakly chaotic case $\bar{F}_{\text{eq}} = 6$, we choose the downward ramp so that the statistical structure will change vastly with an exchange of the dominant mode. Next we consider applying the statistical control on the perturbed L-96 model with scalar control forcing $\kappa(t)$ at different time of the perturbation $\delta F_0(t)$ so that the control skill with different perturbation amplitudes can be tested.

For the numerical method, we use Monte-Carlo simulations with an ensemble size $N = 10000$ to get accurate statistics in mean and variance. To check the control skill with different perturbed initial data, we first apply the ramp-type perturbation in the system, and then replace the forcing with the control at a later time. In general the verification can be carried out according to the following steps:

1) Choose the time T_{ctrl} as the start time to apply control. Then run the original model with original forcing perturbations δF up to the control time T_{ctrl};

2) Use the statistics at time T_{ctrl} as the initial value of the control, and switch the original forcing perturbation δF to the optimal control forcing $\kappa(t)$ from this time as the forcing perturbation;

3) Run the model up to the final time T, and check the model responses in the statistics going back to the unperturbed state as the control $\kappa(t)$ is applied.

3.2.1. Recovering $\kappa(t)$ from optimal control $C(t)$

First we check the recovery of the control forcing $\kappa(t)$ from the inversion problem (2.19) under the L-96 model. $C(t)$ is recovered from the explicit solution in (3.2), then $\kappa(t)$ is found by solving the dynamical equation (2.24) with

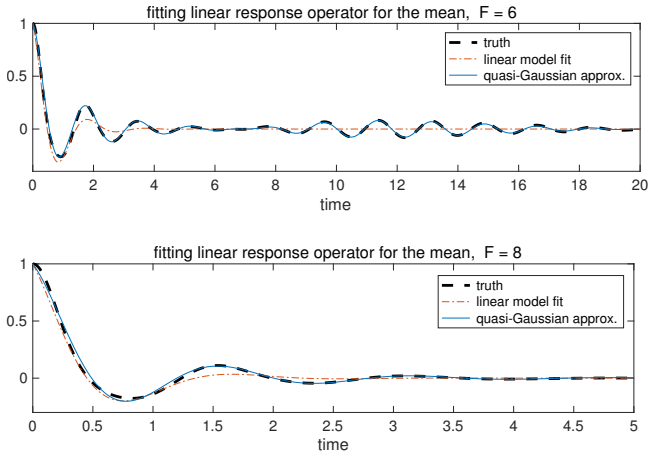

Figure 3.4: Fitting for the linear response operator $\mathcal{R}_{\bar{u}}$ in the mean mode with linear model. The L-96 system is used as the test model in equilibrium regimes $F = 6$ and $F = 8$. The true linear response operator $\mathcal{R}_{\bar{u}}$ (dashed black) is compared with the quasi-Gaussian approximation (2.8) using autocorrelation functions (solid blue), and the linear model fitting $\mathcal{R}^M_{\bar{u}}(t) = \exp(-(d_M + i\omega_M)t)$ with optimal parameter (dotted-dashed red).

optimal model parameter γ_M. In the attribution of the optimal statistical control $C(t)$, only the dominant leading order response in the uniform mean $\bar{u}$ is needed in this simple homogeneous perturbation case. Thus the equilibrium state $\bar{u}_{\rm eq}, \bar{F}_{\rm eq}$ in (2.20) only have real part. Still we find that the autocorrelation functions (2.10) usually display oscillating structures, thus it is useful to introduce a complex coefficient $\gamma_M = d_M + i\omega_M$ in the fitting (2.22) in treating the oscillations. As a result we still solve the 2×2 systeim (2.24) with the imaginary parts of the parameters setting as zero, $C^i = 0, \bar{u}^i = 0, \bar{F}^i = 0$.

The optimal model parameter γ_M for fitting the autocorrealtion function can be achieved easily using the procedure described in Appendix B. It appears that we can achieve quite high accuracy in fitting the autocorrelation function using the linear model approximation for $\mathcal{R}_{\bar{u}}$. As a simple illustration, Figure 3.4 displays the fitting results of the linear response operator in the two typical dynamical regimes $F = 6, 8$ from the equilibrium L-96 model. The true linear response operator for the mean state $\mathcal{R}_{\bar{u}}$ is first compared with the quasi-Gaussian approximation (2.8) using the true autocorrelation functions. Exact recovery can be reached in this homogeneous statistics case of L-96. Then the linear model fit $\mathcal{R}^M_{\bar{u}}(t)$ with optimal parameter still gives good approximation despite some errors in the long time correlation. It will be seen in the controlled responses next that the errors in fitting the autocorrelations will have little effect on the final control performance. (See figures from [19, 20, 28] for some further comparisons in this linear model approximation with the true linear response operator.)

The solutions of the optimal statistical control $C^*(t)$ and control forcing $\kappa(t)$ in the two test cases $\bar{F}_{\rm eq} = 6, 8$ are plotted in Figure 3.5 with changing values of α. The parameter α sets the weight of the control in the cost function $\mathcal{F}_\alpha$. Thus smaller values of α will lead to stronger control forcing κ. First the statistical control $C(t)$ is determined purely based on the dissipative structure of the system thus it acts as a restoring forcing on the total energy fluctuation E. In the strongly non-Gaussian case $\bar{F}_{\rm eq} = 6$, a downward forcing perturbation is added. Thus the total statistical energy will decrease subject to the perturbation. Then a positive control forcing is introduced to drive the system back to equilibrium. On the other hand, in the near-Gaussian case $\bar{F}_{\rm eq} = 8$, upward forcing perturbation increases the total statistical energy. Therefore the control forcing gets negative values. Correspondingly in the final control forcing, different values of parameter α mostly result in the strength at the very beginning of the control time. Especially with small values of α, the control forcing $\kappa(t)$ reverses directions in the control process as a further correction to the strong forcing exerted at the beginning control time. This reflects the oscillatory structure in the autocorrelation function.

3.2.2. Optimal statistical control in major statistical quantities

Next we verify the control performance with the control forcing $\kappa^*(t)$ achieved from the previous optimal statistical control strategy and test it on the L-96 model. In this simple case with homogeneous perturbation, the statistical mean $\bar{\mathbf{u}}$ at each grid point is uniform with the same value $\bar{\mathbf{u}} = \bar{u}\mathbf{e}_0$, and the covariance matrix $R = \left\langle \mathbf{u}'\mathbf{u}'^T \right\rangle$ becomes diagonal.

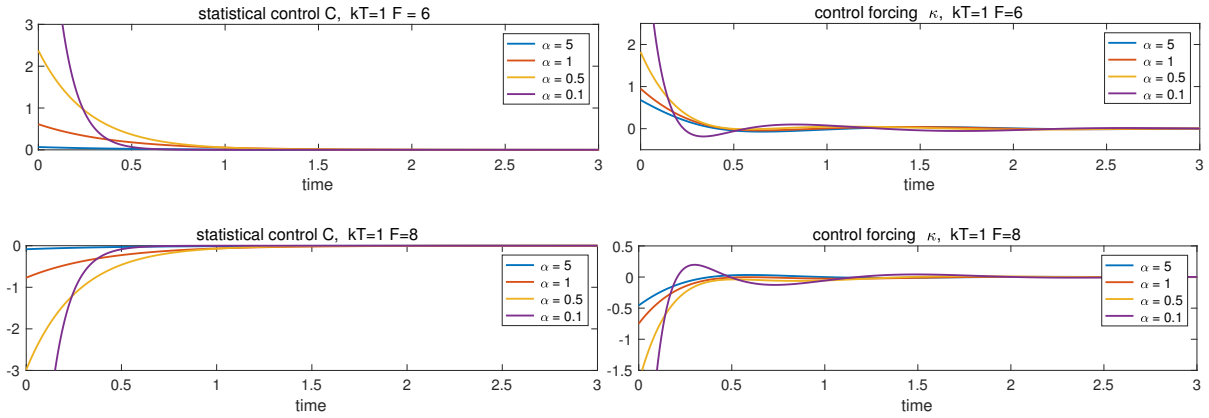

Figure 3.5: Solutions of the optimal statistical control $C^*(t)$ and the control forcing $\kappa^*(t)$ with different parameter values of α in the test regimes $\bar{F}_{\text{eq}} = 6, 8$ of the L-96 model.

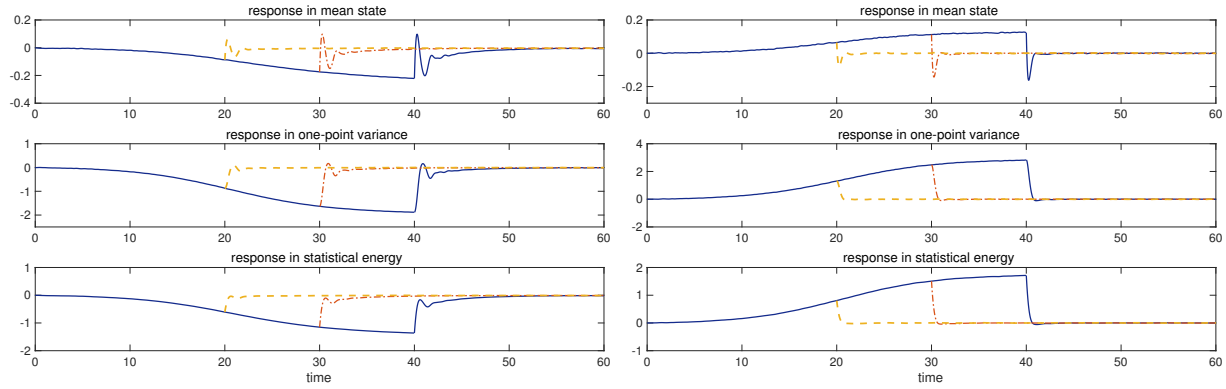

(a) regime with $F = 6$

(b) regime with $F = 8$

Figure 3.6: Comparison of control performance in regime $\bar{F}_{\text{eq}} = 6$, and $\bar{F}_{\text{eq}} = 8$. The control forcing $\kappa(t)$ is applied at different time $T_{\text{ctrl}} = 20, 30, 40$. All the cases use the control model parameter $\alpha = 0.1$.

Thus we may just check three representative statistical quantities, that is, the averaged mean state, $\bar{u} = \frac{1}{J}\sum_{j=1}^{J} \bar{u}_j$; the one-point variance, $r_{1\text{pt}} = \frac{1}{J}\sum_{j=1}^{N} R_{jj}$; and the total statistical energy, $E^{\text{stat}} = \frac{1}{2}\bar{u}^2 + \frac{1}{2}r_{1\text{pt}}$, in the tests for controlled responses. In Figure 3.6, we show the controlled responses in statistical mean, one-point variance, as well as the total statistical energy in the two test regimes $\bar{F}_{\text{eq}} = 6, 8$. The control is applied at various time $T_{\text{ctrl}} = 20, 30, 40$ with the ramp-type perturbation forcing δF_0 so that the control responses with different amplitudes of perturbations can be tested. Especially with large amplitude in the perturbation, the responses in mean may go beyond the linear range of the first order prediction. Still in both test regimes and with different perturbation amplitudes, the control forcing displays the skill in driving the perturbed mean and variance back to the equilibrium state in a rapid rate. Specially in the case with highly non-Gaussian statistics, $\bar{F}_{\text{eq}} = 6$, the forcing perturbation changes the statistical structure of the system greatly. Also notice that oscillation and overshoot in response could be induced especially in the mean state due to the strong nonlinear responses in the system.

3.2.3. Statistical control performance with different parameter values of α

In this simple test case with uniform perturbation δF_0, it enables us to investigate more details in the control strategies depending on the parameter values. In Figure 3.7 we show the controlled responses in the statistical mean state and one-point variance with three different values of the control parameter $\alpha = 0.1, 0.5, 1$. The control begins at time $T_{\text{ctrl}} = 40$ where a large forcing perturbation is exerted. Remember that the parameter α is the weighting

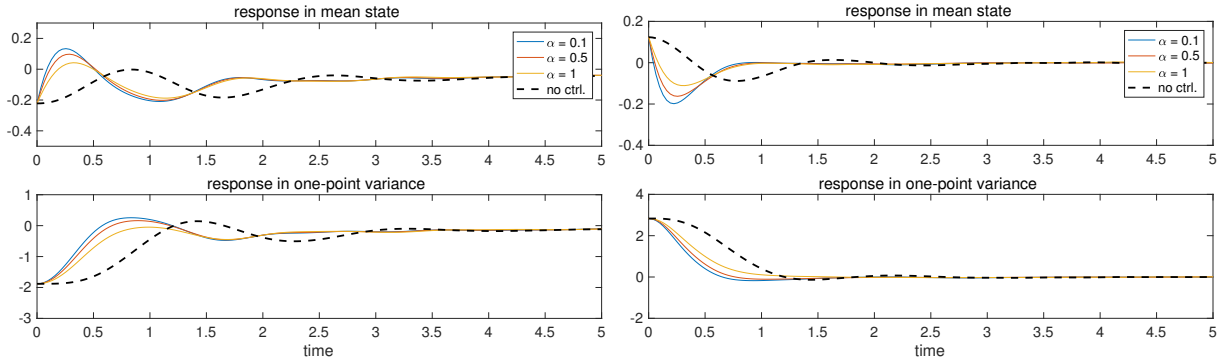

(a) regime with $F = 6$ (b) regime with $F = 8$

Figure 3.7: Comparison of control performance with different values of $\alpha = 0.1, 0.5, 1$ in regime $\bar{F}_{\text{eq}} = 6$, and $\bar{F}_{\text{eq}} = 8$. The uncontrolled case (without adding the control forcing κ after the control time $T_{\text{ctrl}} = 40$) is compared in black dashed lines.

parameter of the statistical control $C(t)$ in the cost function (3.2). Thus smaller values of α will lead to stronger control forcing $\kappa(t)$ in the initial control time. In the figure we first compare all the control results with the uncontrolled case (in dashed lines) where no additional forcing correction is added to the system after the control time T_{ctrl} starts. So it is a 'free drop' case to go back to the unforced equilibrium state in the time scale of the decorrelation time. On the other hand, with the help of the control forcing, both the statistical mean state and the one-point variance can converge to the unperturbed equilibrium in a faster rate. And smaller value of α will offer a faster convergence rate, while it may lead to an overshoot in some extent due to the too strong control forcing exerted at the initial control time as shown in Figure 3.5. Comparing all the controlled responses, medium values of α are already good enough to receive desirable control performance with not too large cost in the control forcing.

4. Linear Statistical Control Model for Inhomogeneous Systems and Perturbations

Previously the simple scenario with control on homogeneously perturbed system is used to illustrate the basic strategy in the efficient statistical control method. In this section we move on to consider the statistical control with additional inhomogeneous effects in perturbations. In the following parts of this section, we propose two representative test models to illustrate the control skill in treating inhomogeneous perturbations. The first model is the 40-dimensional L-96 model that has already been applied for the homogeneous perturbation tests in Section 3 and [17]. As a further application, we introduce small scale inhomogeneous perturbations on top of the original L-96 system. Second, we will consider turbulent topographic barotropic flow, where anisotropy and instability are introduced through topographic stress and rotation effects. Both of the two systems include the representative statistical energy conserving quadratic nonlinearity (especially for the barotropic model, typical triad interactions are crucial for the energy cascades between small and large scale modes).

For example as in the L-96 model, still assume homogeneous statistics in equilibrium (typically we assume homogeneous damping, $D = -dI$, in the dissipation term in the general system (2.1)), so that the mean state maintains a scalar field and the covariance matrix stays diagonal in the unperturbed statistical equilibrium, that is,

$$\bar{\mathbf{u}}_{\text{eq}} = \bar{u}_{\text{eq}}\mathbf{e}_0, \quad R_{\text{eq}} = \text{diag}\left\{r_{1,\text{eq}}, \cdots, r_{N,\text{eq}}\right\}, \quad \mathbf{F}_{\text{eq}} = F_{\text{eq}}\mathbf{e}_0,$$

with the external deterministic forcing F_{eq} also as a scalar applying on the mean state. In the simple case with homogeneous perturbation, $\delta\mathbf{F} = \delta F_0\mathbf{e}_0$, we only need to focus on the responses in the homogeneous mean state, $\delta\bar{u}_0$ (that is, only the $k = 0$ mode needs to be fit in the linear response to get the leading order response).

However in many situations, ***inhomogeneous perturbation*** may not always stay as a higher order quantity, which can strongly affect the perturbed flow structures in the largest scales. For example, inhomogeneity could come from the topographic stress on the bottom topography or from the small scale surface wind drift in realistic models. To

first illustrate the inhomogeneity in the simple model, we introduce the effects from *inhomogeneous perturbations on smaller scale modes* so that

$$\delta\mathbf{F} = \sum_{k\in\Lambda} \delta F_k \mathbf{e}_k + \delta F_0 \mathbf{e}_0, \quad \delta\bar{\mathbf{u}} = \sum_{k=-N}^{N} \delta\bar{u}_k \mathbf{e}_k + \delta\bar{u}_0 \mathbf{e}_0. \tag{4.1}$$

Still $(\delta F_0, \delta\bar{u}_0)$ represent the homogeneous perturbation and mean response like before on the uniform mean mode $\mathbf{e}_0$, while the small scale mode coefficients $(\delta F_k, \delta\bar{u}_k)$ introduce additional perturbations and mean responses from the mode $\mathbf{e}_k$. Above in (4.1) we assume the perturbation $\delta\mathbf{F}$ is applied on a subset of the modes $\Lambda \subseteq \{k \mid |k| \le N\}$, while the mean responses $\delta\bar{\mathbf{u}}$ may spread to the entire spectrum due to the nonlinear interactions between scales. With the inhomogeneous perturbations in (4.1), higher order statistical responses should be included in the original statistical energy equation (2.6). Considering the complete perturbed changes in the fluctuating energy equation, there are the complete form of the feedbacks from deterministic and stochastic forcing

$$\left(\bar{u}_{\mathrm{eq}} \cdot \delta F_0 + \bar{F}_{\mathrm{eq}} \cdot \delta\bar{u}_0\right) + \sum \delta F_k \cdot \delta\bar{u}_k + \sum \sigma_k^2. \tag{4.2}$$

Above the first part is the original leading order terms in the perturbed statistical energy including non-zero equilibrium mean and forcing $\left(\bar{u}_{\mathrm{eq}}, \bar{F}_{\mathrm{eq}}\right)$. In the present discussion since the unperturbed equilibrium is homogeneous, thus only the scalar mean and forcing are included in the leading order part. The second order correction is due to the inhomogeneous responses $\delta\bar{u}_k$ in the transient state. With inhomogeneous perturbation the second order feedbacks may become non-negligible. The final term σ_k^2 is the additional stochastic errors from the linear response approximation of $\delta\bar{u}_k$ to allow for wider applicability to further development.

In constructing a control strategy with inhomogeneous perturbations, nevertheless we still use the same control based on the leading order terms, $\bar{u}_{\mathrm{eq}} \cdot \delta F_0 + \bar{F}_{\mathrm{eq}} \cdot \delta\bar{u}_0$, in the total statistical equation, even though the second order feedbacks in (4.2) might also be important with inhomogeneous perturbations δF_k and mean responses $\delta\bar{u}_k$. In real applications, we may have no access to the exact information about the perturbation structure in each small scale. Thus the robustness of the control method in admitting considerable model errors is a crucial issue to check. In controlling the system with forcing perturbation in the form (4.1), the idea is to propose uniform control forcing $\kappa(t)\,\mathbf{e}_0$ only with homogeneous part to check whether the inhomogeneous responses can also be controlled with this homogeneous control forcing in an efficient way. In this way, the same strategy as in Section 3 can be easily applied to the more complicated case including strong inhomogeneity. As a complement, we briefly discuss and compare the control performance including the second-order nonlinear response $\delta F_k \cdot \delta\bar{u}_k$ in Appendix A.

4.1. Statistical control in L-96 model with inhomogeneous perturbation

In the first test model we use again the L-96 system with 40 grid points as in (3.7) while inhomogeneous forcing perturbation δF_j is added at each grid point

$$\frac{du_j}{dt} = \left(u_{j+1} - u_{j-2}\right) u_{j-1} - u_j + \bar{F}_{\mathrm{eq}} + \delta F_j(t), \quad j = 1, \cdots, J = 40.$$

To introduce inhomogeneity in the external forcing, we consider a small scale perturbation on top of the original uniform forcing

$$\mathbf{F} = \bar{F}_{\mathrm{eq}}\mathbf{e}_0 + \sum_{k\in\Lambda} \delta\bar{F}_k \mathbf{e}_k, \quad \mathbf{e}_k = e^{ik\cdot x}, \tag{4.3}$$

where Λ is a subset of all the spectral modes for the perturbed directions. Fourier modes are used to characterize each small scale due to the periodic boundary condition. The equilibrium forcing is still homogeneous on the mean mode $\mathbf{e}_0$, and the ramp-type forcing is again used for the perturbations on spectral modes changing from zero to the largest value δf_k

$$\delta F_k(t) = \delta f_k \frac{\tanh a(t - t_c) + \tanh a t_c}{1 + \tanh a t_c}.$$

We choose to perturb the most sensitive directions of the model so that large deviations from the equilibrium state can be reached. The model sensitivity to perturbations in each direction can be illustrated by the integration of

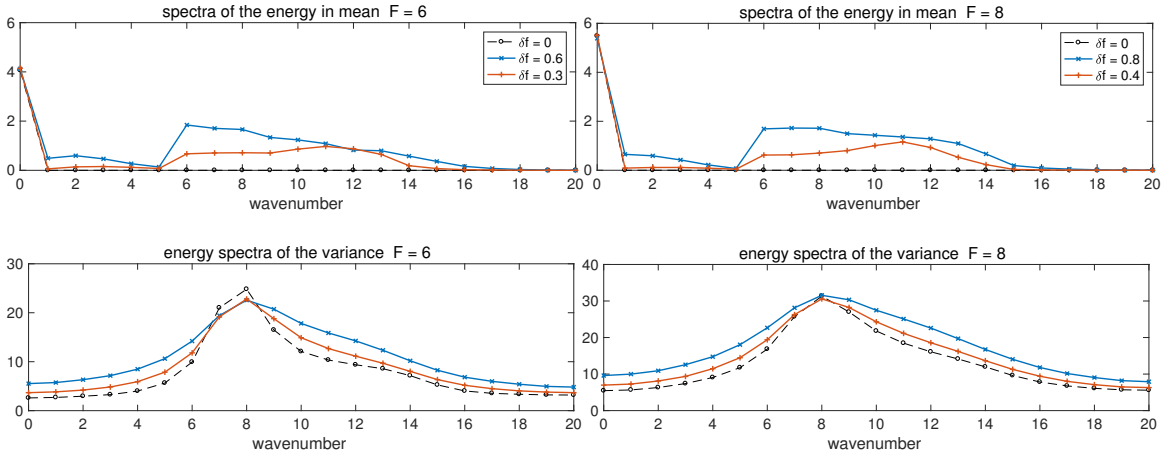

Figure 4.1: Spectra of energy in the mean $|\bar{u}_k|^2$ and variance $\overline{|u'_k|^2}$ in the inhomogeneous perturbed case of L-96 system in regimes $F = 6, 8$. δf is the amplitude of the inhomogeneous perturbation in each mode.

autocorrelation functions $\mathcal{R}_k(t) = \langle u_k(t)\, u_k(0)\rangle$ [23, 22]. In general in L-96 system, the modes with largest energy $k = 6, 7, 8, 9, 10$ are highly oscillatory with largest absolute decorrelation time $\int_0^\infty |\mathcal{R}_k(t)|\, dt$; on the other hand, modes $k = 11, 12, 13, 14$ get the longest decorrelation time $\left|\int_0^\infty \mathcal{R}_k(t)\, dt\right|$ thus become the most sensitive directions [22, 23].

In our test case, we add perturbation on both the high energy modes $k = 6, 7, 8, 9, 10$ (with largest absolute decorrelation time) and most sensitive modes $k = 11, 12, 13, 14$ (with largest decorrelation time). Thus the perturbed subset of modes contains $k \in \Lambda = \{6, 7, 8, 9, 10, 11, 12, 13, 14\}$ compared with the full spectrum with 20 complex modes. The largest amplitude of small scale perturbation is set as $\delta f_k = 0.1\bar{F}$ at each small scale mode. Figure 4.1 shows the energy in the mean, $|\bar{u}_k|^2$, and the variance, $\overline{|u'_k|^2}$ in each spectral mode in the two test regimes with equilibrium forcing $\bar{F}_{\rm eq} = 6, 8$. The spectra with two perturbation forcing amplitudes $\delta f_k = 0.05\bar{F}, 0.1\bar{F}$ are compared. Unlike the homogeneous perturbation case with no exited small scale mean, many mean modes in small scales get non-zero values due to the inhomogeneous forcing while the change in the uniform mean state $\bar{u}_0$ is small. In the spectra for variance, more modes become energetic due to the inhomogeneous forcing at the same time.

4.1.1. Linear statistical control strategy in the L-96 system

In testing the control performance in this inhomogeneous perturbation case, we still follow the general control formulation in Section 2 and apply the strategy to the inhomogeneously perturbed system (4.3) in L-96 model. The total statistical energy equation (2.13) for L-96 by taking $d = 1$ and with control only on the single uniform mode then becomes

$$\frac{dE}{dt} = -2E(t) + C(t), \quad E(t) = \frac{1}{2}\sum_{j=1}^{J}\left(\bar{u}_j^2 + \overline{u_j'^2}\right) - E_{\rm eq}, \tag{4.4}$$

where the energy fluctuation $E(t)$ contains the total first and second order moments in all the $J = 40$ modes. The equilibrium total statistical energy $E_{\rm eq}$ can be determined purely by the statistical mean state with homogeneity

$$2E_{\rm eq} = \bar{u}_{\rm eq}\bar{F}_{\rm eq}, \quad \bar{u}_j \equiv \bar{u}_{\rm eq} \text{ for all } j.$$

In the exact form, the statistical control $C(t)$ should include both linear and nonlinear responses due to inhomogeneous perturbations as in (4.2). Solving statistical control of C in the first stage does not concern about the explicit forms in the statistical mean feedbacks. Thus this single statistical control C can be solved in the same way as the explicit solution in (3.2) with the scalar Riccati equation.

In the second stage we consider the statistical inversion of inhomogeneous perturbation problem. Still we only use the leading order part in finding the control forcing $\kappa(t)$

$$C(t) = \bar{u}_{\rm eq}\kappa(t) + \bar{F}_{\rm eq}\mathcal{L}_{\bar{u}}(t). \tag{4.5}$$

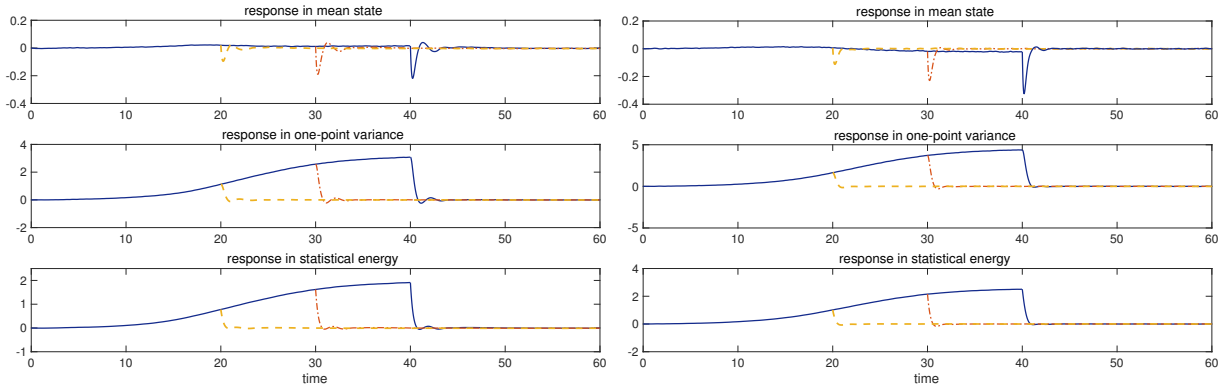

(a) $F = 6$ (b) $F = 8$

Figure 4.2: Linear statistical control in regimes $F = 6$ and $F = 8$ in L-96 system with inhomogeneous perturbation (4.3). Controlled responses in statistical mean and one-point variance at different control time $T_{\text{ctrl}} = 20, 30, 40$ using the control forcing are compared with parameter value $\alpha = 0.1$.

So only a homogeneous control forcing $\vec{\kappa}(t) = \kappa(t)\,\mathbf{e}_0$ is applied to this inhomogeneously perturbed system. Keep in mind that the exact forms of the total statistical control $C(t)$ should include non-zero second order feedbacks from all the perturbed small-scale modes, $\delta\bar{u}_k \cdot \delta F_k$. We only use linear first order response considering that: i) the linear response in the mean state is approximated by linear model

$$\mathcal{L}_{\bar{u}}(t) = \int_0^t \mathcal{R}_{\bar{u}}(t-s)\,\kappa(s)\,ds = \int_0^t e^{-\gamma_M(t-s)}\kappa(s)\,ds,$$

thus the error from the leading order linear response approximation $\delta\bar{u}$ could be dominant; and ii) it has been shown that the control method is quite robust in performance even with large model errors. Thus it is useful to check whether acceptable control performance can be achieved with even this crude approximation. If possible, more detailed calibration with higher order responses might be unnecessary in many cases which could be much more expensive in computation. Considering all these aspects, the control forcing $\kappa(t)$ can be recovered using exact same strategy by solving the system (2.24) as in Section 2. In summary, we use exactly the same strategy as the homogeneous perturbation case, but apply it to the system with inhomogeneous perturbations.

4.1.2. Verification of the control in L-96 system with inhomogeneous perturbation

To show the control performances with different perturbation amplitudes, the inhomogeneous perturbation (4.3) with a ramp-type forcing is applied first to the original L-96 model and the control forcing is added at different control time $T_{\text{ctrl}} = 20, 30, 40$. Figure 4.2 shows the control responses in statistical mean $\bar{u} = \frac{1}{J}\sum_{j=1}^{J}\bar{u}_j$, the one-point variance, $r_{1\text{pt}} = \frac{1}{J}\text{tr}R$, and the total statistical energy, $E^{\text{stat}} = \frac{1}{2}\bar{u}^2 + \frac{1}{2}r_{1\text{pt}}$, in the two test regimes with equilibrium forcing $\bar{F}_{\text{eq}} = 6, 8$. With inhomogeneous forcing perturbation along the small scale modes, the changes in the averaged mean state are small. On the other hand, we apply homogeneous control forcing $\kappa(t)$ directly on the base mode, thus small fluctuations can be induced in the mean responses after the control forcing is applied at the beginning control time. The single-point variance and total statistical energy converge to the unperturbed state in a rapid rate in both dynamical regimes. Overall the control results are generally good among all the different perturbation amplitudes even with only first-order homogeneous control forcing in this inhomogeneous perturbation case. In the control process, we always take the parameter value $\alpha = 0.1$. Smaller parameter values of α will lead to stronger control forcing in the initial control time and more rapid decay in the forcing as discussed before in Section 3.2.

In this inhomogeneous perturbation case, the perturbations are added in a subset $\Lambda = \{6, 7, 8, 9, 10, 11, 12, 13, 14\}$ of all the small scale modes. Next it is useful to check in detail about the responses in the perturbed modes among the subset Λ and in the rest unperturbed directions. Figure 4.3 shows the statistical responses of the energy in the mean and variance among the perturbed modes, $\sum_{k\in\Lambda}|\hat{u}_k|^2$, and in the rest unperturbed subspace, $\sum_{k\in\Lambda^c}|\hat{u}_k|^2$. In both

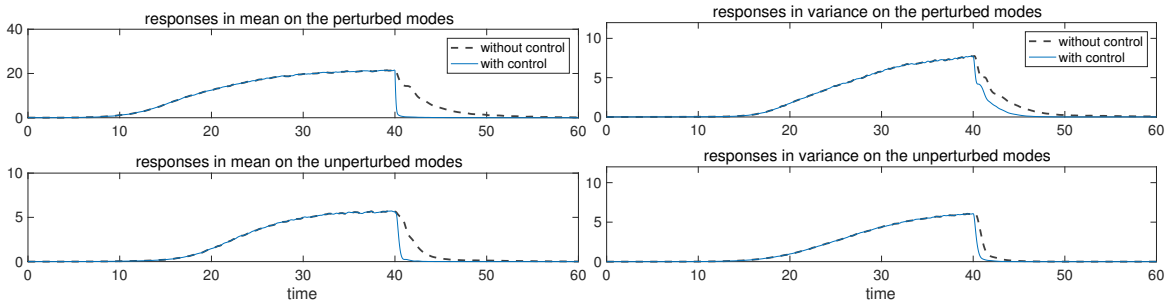

(a) $F = 6$

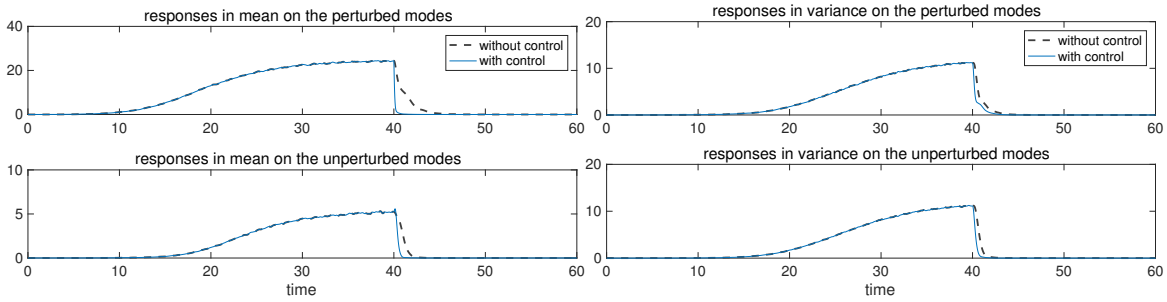

(b) $F = 8$

Figure 4.3: Controlled responses in statistical energy in mean and variance among the perturbed modes and unperturbed modes. Perturbations are added among a subset of the Fourier modes $\Lambda = \{6, 7, 8, 9, 10, 11, 12, 13, 14\}$, and homogeneous control forcing $\kappa(t)$ is applied on the uniform mean state. The results with the control forcing are compared with the uncontrolled case without forcing after the control time.

the test regimes with $\bar{F} = 6, 8$, the perturbed subspace gets stronger responses in both mean and variance while there are also changes in the unperturbed subspace due to the nonlinear transfer of energy between modes. In this strategy with homogeneous control forcing, we only add a scalar uniform control forcing $\kappa(t)$ to the system despite that the major part of the perturbations is added on the smaller scale modes (in both perturbed and unperturbed subspace). The uniform control forcing guarantees the effectively control on all the small scale modes to the equilibrium state in a much faster rate in both the perturbed and unperturbed subspace especially in the mean state.

Finally we also check the responses in the mean state and variance in each individual mode in the two test regimes $\bar{F} = 6, 8$ in Figure 4.4 and 4.5. Remind that the uniform control forcing κ is not applied on these small scale modes directly, whereas the responses in these modes can be controlled through the interaction with the mean state that is directly controlled by the forcing. Again compared with the uncontrolled case without the effect of control forcing after the control time, the controlled case achieves faster convergence rate back to the equilibrium in each single perturbed mode in both the statistical mean state and variance. Still, especially for the $F = 6$ case, some oscillating structures are developed after the control is applied. This is due to the strong non-Gaussian effect and long decorrelation time dominant in this regime. Together these fast convergences in the perturbed states show the effectiveness and robustness of the simple statistical control strategy focusing on the mean statistical responses.

Remark. In contrast with the first-order control only using the leading order terms in the total statistical equation expansion in (4.2), an interesting question is what is the effects of including the second-order responses, $\delta F_k \cdot \delta \bar{u}_k$, in the control process. In Appendix A, we develop control models taking into account the second-order contributions to introduce an inhomogeneous control forcing, $\vec{\kappa}(t)$. It shows that the second-order control on each small scale modes gives similar performance as in Figure 4.4 and 4.5, while the computational costs are much higher since the control forcing along each mode needs to be considered.

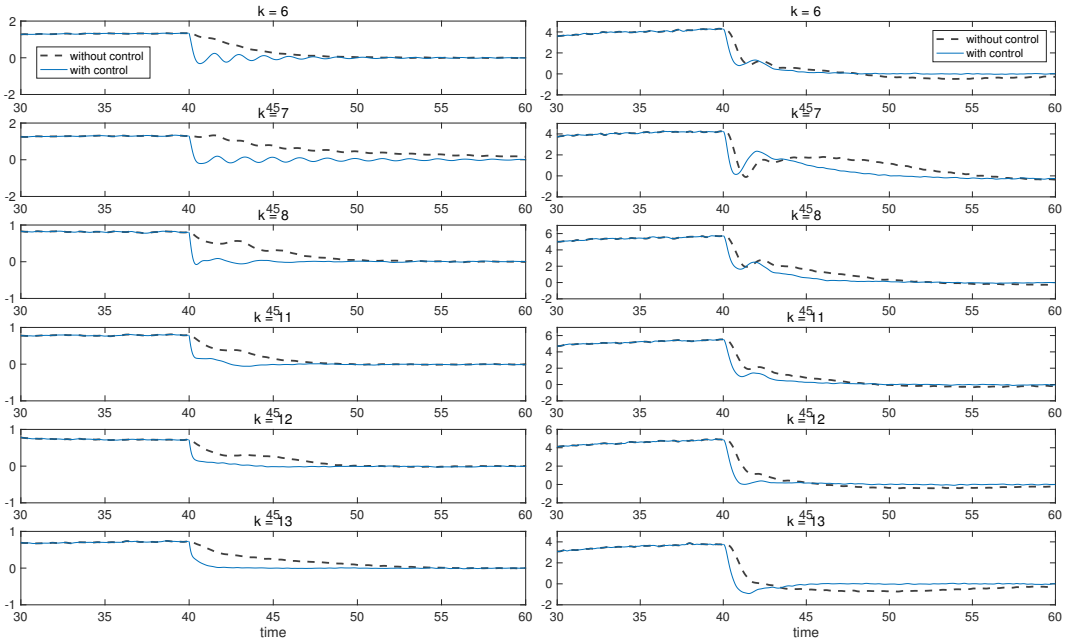

(a) responses in mean state (b) responses in variance

Figure 4.4: Responses in each perturbed spectral mode in statistical mean and variance in regime $\bar{F} = 6$ in the inhomogeneous perturbed case with homogeneous control forcing. Responses in most sensitive directions are selected. The uncontrolled case after the control time $T_{\text{ctrl}} = 40$ is shown in dashed lines.

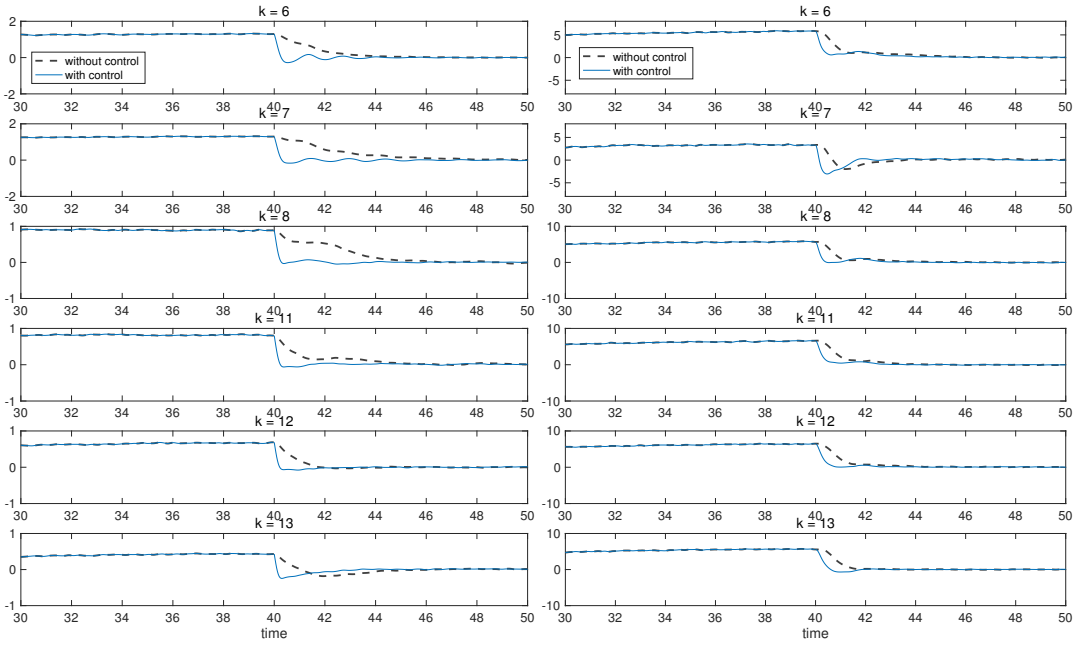

(a) responses in mean state (b) responses in variance

Figure 4.5: (Continuing) Responses in each perturbed spectral mode in statistical mean and variance in regime $\bar{F} = 8$ in the inhomogeneous perturbed case.

4.2. Statistical control in barotropic flow with topography

In the second test model for control in more realistic inhomogeneous flows, we apply the statistical control strategy in a geophysical barotropic system involving anisotropic and inhomogeneous dynamics. The barotropic flow can be viewed as a vertically averaged one-layer system which generates many interesting and representative features found in the real atmosphere and ocean [13, 12, 30]. Comparing with the stereotype L-96 system, the barotropic model incorporates the essential structures in realistic geostrophic turbulence with a large-scale zonal mean flow U and topographic effect h [12, 21]. In general, the topographic barotropic flow on a rotational β-plane with dissipation and forcing can be formulated in terms of small-scale vorticity and a large-scale mean flow as

$$\begin{aligned} \frac{\partial \omega}{\partial t} + \mathbf{v}\cdot\nabla q + \beta\frac{\partial \psi}{\partial x} + U\frac{\partial q}{\partial x} &= -d\omega + \mathcal{F}(\mathbf{x},t) + \Sigma(\mathbf{x})\dot{W}(t), && (4.6a)\\ \frac{dU}{dt} + \oint \frac{\partial h}{\partial x}\psi(t) &= -dU + \mathcal{F}_0(t) + \Sigma_0\dot{W}_0(t), && (4.6b) \end{aligned}$$

where $q = \omega + h$, $\omega = \Delta\psi$ represent the potential vorticity and relative vorticity respectively; and ψ is the flow stream function; h is the topographic structure while q is advected by the velocity field of the flow, $\mathbf{v} = \nabla^{\perp}\psi \equiv \left(-\partial_y\psi, \partial_x\psi\right)$. The right hand sides are the dissipation (by Ekman damping) and forcing (in both deterministic and stochastic part) terms.

In solving the above barotropic equations in (4.6) with periodic boundary condition, a finite-dimensional truncation is made by applying a Galerkin projection on each Fourier mode $\mathbf{e}_{\mathbf{k}} = \exp(i\mathbf{k}\cdot\mathbf{x})$, where the equations are projected into a subspace with high wavenumber truncation. Consider the Galerkin projection operator $\mathcal{P}_N$ on a subspace with the mean flow U and vorticity mode wavenumbers $1 \le |\mathbf{k}| \le N$, $\mathcal{P}_N(U(t), \omega(\mathbf{x},t)) = (U(t), \omega_N(\mathbf{x},t))$, applied to the original model for topographic barotropic flow (4.6) with the specific forcing and Ekman damping terms

$$\begin{aligned} \frac{d\hat{\omega}_{\mathbf{k}}}{dt} &= -\mathcal{P}_N\left(\nabla^{\perp}\psi_N\cdot\nabla q_N\right)_{\mathbf{k}} + ik_x\left(\beta|\mathbf{k}|^{-2} - U\right)\hat{\omega}_{\mathbf{k}} - ik_x\hat{h}_{\mathbf{k}}U && (4.7a)\\ &\quad -d\hat{\omega}_{\mathbf{k}} + \sigma_{\mathbf{k}}\dot{W}_{\mathbf{k}} + \bar{F}_{\mathbf{k}} + \delta F_{\mathbf{k}}, \qquad 1 \le |\mathbf{k}| \le N,\\ \frac{dU}{dt} &= -\sum_{1\le|\mathbf{k}|\le N} ik_x|\mathbf{k}|^{-2}\hat{h}^*_{\mathbf{k}}\hat{\omega}_{\mathbf{k}} - dU + \sigma_0\dot{W}_0 + \bar{F}_0 + \delta F_0. && (4.7b) \end{aligned}$$

Above $\hat{\omega}_{\mathbf{k}}$ is the Fourier coefficient of the flow vorticity ω on the projected model. Only linear Ekman friction is introduced in the dissipation term. The stochastic noise is defined in each mode as, $\sigma_0 = \sigma|\mu|^{-1/2}$, $\sigma_{\mathbf{k}} = \sigma\left|1 + \mu|\mathbf{k}|^{-2}\right|^{-1/2}$ with the parameter μ. Only small noise is needed to guarantee ergodicity of the system [16]. In the regime with $\mu > 0$, it can be shown that this random noise can maintain a Gaussian invariant measure in statistical equilibrium and the system is stable through nonlinear stability theory [20, 21]. The equilibrium deterministic forcing $\left(\bar{F}_0, \bar{F}_{\mathbf{k}}\right)$ is introduced in consistency with the climatology $\left(\bar{\omega}_{\mathrm{eq}}, \bar{U}_{\mathrm{eq}}\right)$ as

$$\bar{F}_{\mathbf{k}} = d\bar{\omega}_{\mathrm{eq},\mathbf{k}}, \quad \bar{F}_0 = d\bar{U}_{\mathrm{eq}}. \tag{4.8}$$

Usually the equilibrium state $\left(\bar{\omega}_{\mathrm{eq}}, \bar{U}_{\mathrm{eq}}\right)$ is defined with the model parameter μ through a linear dependence between the stream function and potential vorticity [12, 21, 20]

$$\bar{U}_{\mathrm{eq}} = -\frac{\beta}{\mu}, \quad \bar{\omega}_{\mathrm{eq},\mathbf{k}} = -\frac{|\mathbf{k}|^2\hat{h}_{\mathbf{k}}}{\mu + |\mathbf{k}|^2}. \tag{4.9}$$

The unperturbed equilibrium mean (4.9) and forcing (4.8) get inhomogeneous structure due to the topography h. In the numerical tests, we will consider two typical parameter values, $\mu = 2$ and $\mu = -0.5$, thus the large scale mean flow $\bar{U}_{\mathrm{eq}}$ gets opposite directions in steady state. The additional forcing terms $(\delta F_0, \delta F_{\mathbf{k}})$ represent the potential external perturbations added on the system driving the state variables away from the original equilibrium state. More statistical features about the truncated barotropic flow (4.7) are investigated in detail in [16, 21, 20].

4.2.1. Control of the barotropic model using conservation of statistical energy

In controlling the topographic barotropic system, we assume that the equilibrium statistical mean state $\left(\bar{U}_{\rm eq}, \bar{\omega}_{\rm eq}\right)$ (i.e. the climate) is known with reasonable accuracy, and the goal is to find the optimal control (as one external forcing) that can drive the perturbed states (say, due to climate change) back to the equilibrium at a fast rate. In this specific control problem about the perturbed system with $(\delta F_0, \delta F_{\mathbf{k}}) \neq 0$ in (4.7), the task is to design a proper control forcing $\kappa(t)$ driving the perturbed system back to the original unperturbed equilibrium states $\left(\bar{U}_{\rm eq}, \bar{\omega}_{\rm eq}\right)$. As the general framework discussed in Section 2, we would like to begin with a scalar statistical dynamical equation (2.3) according to the proper conserved quantity to derive a optimal statistical control $C(t)$ as in (2.12). Then the standard procedure can be used to find the optimal control by solving a scalar Riccati equation regardless of the complicated nonlinear effects contained in the complex system.

For the topographic barotropic flow (4.6) with mean flow, both the total energy, $\frac{1}{2}U^2 + \frac{1}{2}\int |\nabla\psi|^2$, and the large-scale enstrophy, $\beta U + \frac{1}{2}\int \omega^2$, stay conserved due to the symmetry in the nonlinear interactions, $\nabla^\perp\psi \cdot \nabla q$ [12, 21]. Here, we use the conservation of total energy in the statistical control and consider the statistical energy dynamics following the general framework in [15, 16]. Therefore define the fluctuation of total statistical energy about the equilibrium state

$$E^{\rm stat} \quad = \quad E_0^{\rm stat} + \sum_{\mathbf{k}\neq 0} E_{\mathbf{k}}^{\rm stat}, \tag{4.10}$$

$$E_0^{\rm stat} = \frac{1}{2}\mathbb{E}U^2 - \frac{1}{2}\mathbb{E}U_{\rm eq}^2, \quad E_{\mathbf{k}}^{\rm stat} = \frac{1}{2}\mathbb{E}\,|\mathbf{k}|^2\,|\psi_{\mathbf{k}}|^2 - \frac{1}{2}\mathbb{E}\,|\mathbf{k}|^2\left|\psi_{{\rm eq},\mathbf{k}}\right|^2,$$

where $\mathbb{E}x^2 = \bar{x}^2 + \overline{x'^2}$ represents the statistical energy of the random process x combining the statistics in mean and variance together, and $U_{\rm eq}, \psi_{\rm eq}$ are the state variables in the unperturbed equilibrium with $\delta F_0 = 0, \delta F_{\mathbf{k}} = 0$. The statistical energy (4.10) only contains the perturbed fluctuation part away from the equilibrium. It is easy to check that the nonlinear terms in (4.7) will not change the total statistical energy $E^{\rm stat}$. The dynamical equation for the statistical energy in (4.10) can be derived as a special form according to the general formulation (2.6) of the control problem in Section 2

$$\frac{dE^{\rm stat}}{dt} = -2dE^{\rm stat} + \left(\bar{F}_0 \cdot \delta\bar{U} + \bar{U}_{\rm eq} \cdot \delta F_0\right) + \sum_{\mathbf{k}} |\mathbf{k}|^{-2}\left(\bar{F}_{\mathbf{k}}^* \cdot \delta\bar{\omega}_{\mathbf{k}} + \bar{\omega}_{{\rm eq},\mathbf{k}}^* \cdot \delta F_{\mathbf{k}}\right) + O\left(\delta^2\right). \tag{4.11}$$

Above $\left(\bar{F}_0, \bar{F}_{\mathbf{k}}\right)$ are the deterministic forcing without perturbation, $\left(\bar{U}_{\rm eq}, \bar{\omega}_{\rm eq}\right)$ are the statistical mean in the unperturbed equilibrium, and $\left(\delta\bar{U}, \delta\bar{\omega}_{\mathbf{k}}\right)$ are the first order responses in statistical mean states. On the right hand side of (4.11), additional weight $|\mathbf{k}|^{-2}$ based on the energy inner product is introduced in the feedbacks of the interaction with mean response. Still in the control process we focus on the leading order feedbacks despite the various inhomogeneous perturbation forcing $\delta F_{\mathbf{k}}$.

Specifically in setting the forcing and dissipation part, we consider linear Ekman damping, $-d\omega$, so that the statistical energy equation becomes linear and is easy to solve directly. From (4.6b) the topographic stress in the large scale flow U is only dependent on the zonal variability of h, thus we use simple topography only varying along large-scale x-direction

$$h = H(\cos x + \sin x) = \frac{H}{2}\left[(1-i)\,e^{ix} + (1+i)\,e^{-ix}\right]. \tag{4.12}$$

Then the topographic forcing is only applied on the largest scale zonal modes $\hat{\omega}_{(1,0)}, \hat{\omega}_{(-1,0)}$. Correspondingly, the forcing perturbation is only applied on the mean flow and topographically forced modes,

$$\begin{aligned} &\delta F_0, && \text{on mean flow } U;\\ &\delta F_1, && \text{on topographic mode } \hat{\omega}_{(1,0)}e^{ix};\\ &\delta F_{-1}, && \text{on topographic mode } \hat{\omega}_{(-1,0)}e^{-ix}. \end{aligned}$$

These are the first modes that are most sensitive to external perturbations. One representative feature in the flow field is the shifting directions of the zonal mean flow as the external forcing increases in amplitude.

The control solution with the above model setup is then developed following the general the two-step framework discussed in Section 2. The control on the total statistical energy fluctuation in (4.11) gets the dynamical equation due

to control C_0 on the mean flow U and C_1 on the ground vortical mode ω_1 with $|\mathbf{k}| = 1$

$$\frac{dE^{\text{stat}}}{dt} = -2dE^{\text{stat}} + 2C_1 + C_0. \tag{4.13}$$

Note that the contributions from the two modes $\delta F_{-1} = \delta F_1^*$ are conjugate with each other thus would offer the same contribution in C_1. With the non-zero equilibrium mean (4.9) and forcing (4.8), multiple controls (κ_0, κ_1) should be introduced for all the perturbed directions instead of the previous homogeneous case. Putting all the statistical solutions together as in (2.20) the control forcing $\kappa(t)$ can be recovered together from the implicit relation in a 3×3 system

$$C(t) = \begin{bmatrix} C_0 \\ C_1^r \\ C_1^i \end{bmatrix} = \Omega\mathcal{K} + \Gamma\mathcal{L}_{\bar{u}}, \quad \mathcal{K}(t) = \begin{bmatrix} \kappa_0 \\ \kappa_1^r \\ \kappa_1^i \end{bmatrix}, \ \mathcal{L}_{\bar{u}}(t) = \begin{bmatrix} \delta\bar{U} \\ \delta\bar{\omega}_1^r \\ \delta\bar{\omega}_1^i \end{bmatrix} \ \Omega = \begin{bmatrix} \bar{U}_{\text{eq}} & & \\ & \bar{\omega}_{\text{eq},1}^r & \bar{\omega}_{\text{eq},1}^i \\ & -\bar{\omega}_{\text{eq},1}^i & \bar{\omega}_{\text{eq},1}^r \end{bmatrix}, \ \Gamma = \begin{bmatrix} \bar{F}_0 & & \\ & \bar{F}_1^r & \bar{F}_1^i \\ & -\bar{F}_1^i & \bar{F}_1^r \end{bmatrix}. \tag{4.14}$$

Above $\kappa_0 = \delta F_0$ is the (real) control on the mean flow U, and $\kappa_1 = \delta F_1$ is the (complex) control on the ground mode $\hat{\omega}_{(1,0)}$. The coefficient matrices (Ω, Γ) are determined from the equilibrium statistics in (4.8) and (4.9). Using the same strategy as in Section 2.2.2 to decompose the complex component into real and imaginary part, we avoid the difficulty in treating complex values in numerical implementation. Especially this system (4.14) could be coupled together through the linear response $\mathcal{L}_{\bar{u}}[\kappa_0, \kappa_1]$ mixing the effects from all the control forcing. Still we need to propose the imaginary part of the statistical control C_1. One easy choice is just to take $C_1^r = C_1$ and $C_1^i = 0$ from the statistical control solution.

The statistical control (C_0, C_1) in (4.13) can be purely determined depending only on the dissipation effect of the system. In solving the control problem of the total statistical energy in (4.13), we avoid the complicated nonlinear interactions in the original system in the first stage and introduce the statistical control only based on the dissipation structure (say, $-2dE$ in this case) of the system. The solution is directly from the strategy in Section 2 using the scalar Riccati equation (3.1) in exactly the same form

$$\begin{aligned} \frac{dK}{dt} &= -1 + 4dK(t) + \alpha^{-1}K^2(t), \\ K(T) &= 1, \qquad 0 < t < T. \end{aligned}$$

The optimal energy control can be found from the solution $K(t)$ of the above equation

$$C_0 = -\alpha_0^{-1}K(t)E^{\text{stat}}(t), \quad C_1 = -\alpha_1^{-1}K(t)E^{\text{stat}}(t).$$

The values of α_0, α_1 can be determined by the energy in mean flow U and mode $\hat{\omega}_{(1,0)}$. Using the principle proposed in (2.18) in choosing the weights, one proper choice is to set $\alpha_0 = \alpha w_0^{-1}, \alpha_1 = \alpha w_1^{-1}$ according to the equilibrium variance in the corresponding mode, $w_0 \propto r_{U,\text{eq}}, w_1 \propto r_{\omega_1,\text{eq}}$, so that we only need one single parameter $\alpha > 0$ for the control strength.

4.2.2. Linear approximation for autocorrelation functions in perturbed modes

The next task is to recover the explicit control forcing $\kappa(t)$ with the inversion relation (4.14) through the statistical control solutions C_0, C_1. Still, we can approximate the first-order response $\mathcal{L}_{\bar{u}}$ using linear response theory, that is,

$$\begin{aligned} \delta\bar{U}(t) = \mathcal{L}_U(t) &= \int_0^t \mathcal{R}_U(t-s)\kappa(s)\,ds + O\left(\delta^2\right), \\ \delta\bar{\omega}_1(t) = \mathcal{L}_\omega(t) &= \int_0^t \mathcal{R}_\omega(t-s)\kappa(s)\,ds + O\left(\delta^2\right). \end{aligned}$$

In general, the linear response operators for the mean state $(\mathcal{R}_U, \mathcal{R}_\omega)$ will again include the feedbacks from all the perturbed modes and also non-Gaussian effects (such as, $\langle U(t)\omega_k(0)\rangle$ and $\langle \omega_k(t)\omega_l(0)\rangle$) [20]. Following the strategy in (2.22) in Section 2.2.2, we estimate the linear response operators using a single autocorrelation function as

$$\mathcal{R}_U(t) \sim \langle U(t)U(0)\rangle, \quad \mathcal{R}_\omega(t) \sim \langle \omega_1(t)\omega_1^*(0)\rangle. \tag{4.15}$$

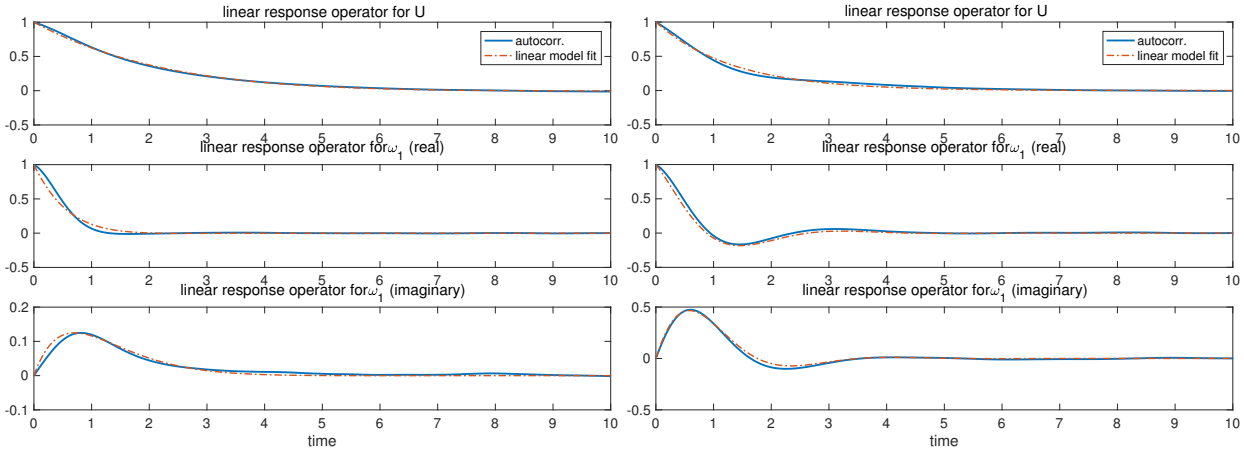

(a) $\mu = -0.5$ (b) $\mu = 2$

Figure 4.6: Linear response operators $(\mathcal{R}_U, \mathcal{R}_\omega)$ for the mean responses in large-scale flow and first vortical mode. The solid blue lines are the autocorrelations for each mode; the dotted-dashed red lines are the linear model fits.

The control on the mean flow U and on the first vortical mode ω_1 in (4.14) is decoupled through this assumption in the diagonalized linear response operators. Then linear model approximations can be used to fit the autocorrelations in the mean and first vortical mode with the parameters $\left(\gamma^M, \omega^M\right)$ as a damping and rotation factor

$$\mathcal{R}_U^M(t) = \exp\left(-\gamma_0^M t\right), \quad \mathcal{R}_\omega^M(t) = \exp\left(-\left(\gamma_1^M - i\omega_1^M\right)t\right). \tag{4.16}$$

Notice that $\mathcal{R}_U$ only has real part for the linear responses of the mean flow U, while $\mathcal{R}_\omega$ contains real and imaginary components. In consistency with the matrix representation in (4.14) the three components of the linear mean responses of interest can be put together using the trick in Section 2.2.2,

$$\Gamma \frac{d}{dt}\mathcal{L}_{\bar{u}} = \Gamma\kappa(t) + \Gamma_1 \mathcal{L}_{\bar{u}},$$

with $\mathcal{L}_{\bar{u}} = \left(\delta\bar{U}, \delta\bar{\omega}_1^r, \delta\bar{\omega}_1^i\right)^T$ and the operator Γ_1 due to the derivative of the response operator

$$\Gamma_1 = \begin{bmatrix} -\gamma_0^M \bar{F}_0 & & \\ & -\gamma_1^M \bar{F}_1^r + \omega_1^M \bar{F}_1^i & -\gamma_1^M \bar{F}_1^i - \omega_1^M \bar{F}_1^r \\ & \gamma_1^M \bar{F}_1^i + \omega_1^M \bar{F}_1^r & -\gamma_1^M \bar{F}_1^r + \omega_1^M \bar{F}_1^i \end{bmatrix}.$$

As an illustration in the fitting process, Figure 4.6 plots the linear response operators and the linear regression model fits in the two test regimes that will be detailed next in Section 4.2.3. The solid lines are the autocorrelation functions in (4.15) for the mean flow U and the first spectral mode ω_1, and the dotted-dashed lines are the linear model fits from the simple approximation using optimal model parameters $\left(\gamma^M, \omega^M\right)$ in (4.16). Good agreement can be achieved by just using the simple fitting method. Still large errors may exist in the single autocorrelation approximation (4.15) for the linear response operators compared with the truth. This is due to the strong inhomogeneous feedbacks in the system from cross-covariances. On the other hand thanks to the robustness of the control method, as we will observe in the control results later, using the parameters with error by just fitting the autocorrelations can already get good control performance in the model, regardless of the relatively large error in the linear response operators in $(\mathcal{R}_U, \mathcal{R}_\omega)$.

Finally the explicit control forcing $\kappa_0(t)$ (for the mean flow U) and $\kappa_1(t) = \kappa_1^r(t) + i\kappa_1^i(t)$ (for the first vorticity mode $\hat{\omega}_{(1,0)}$) can be recovered in the same way of the general formula (2.24) by solving the 3×3 dynamical system

$$\frac{d\kappa}{dt} + \left(\Omega^{-1}\Gamma - \Omega^{-1}\Gamma_1\Gamma^{-1}\Omega\right)\kappa + \Omega^{-1}\left(\Gamma_1\Gamma^{-1} + \left(K^{-1} - 2d\right)I\right)C = 0, \tag{4.17}$$

with the solution $\kappa = \left(\kappa_0, \kappa_1^r, \kappa_1^i\right)^T$. The coefficients are defined from the equilibrium statistics in (4.14). Despite the complex matrix representation this is just a first order linear equation, thus the solution is easy to achieve through numerical integration.

4.2.3. Verification of the control in barotropic model with non-zero mean state

In the numerical simulations, we consider the control model (4.7) with a small wavenumber truncation $|\mathbf{k}| \leq N = 17$ resulting in a total 57 degrees of freedom. This model has the attractive features of the low-order truncated model being exactly like the three-dimensional Charney–DeVore model [31], and consists of a well-defined mean climate state and topographic Rossby waves [16, 21, 20]. A pseudo-spectral scheme is used to integrate the topographic barotropic equation with time step $\Delta t = 0.001$, which is small enough to capture all the small-scale dynamics. No additional hyperviscosity is needed in this small truncation case with only low wavenumbers included. We verify the control skill for the topographic barotropic flow under the following model parameter setups:

- The unperturbed equilibrium case is assumed with no additional forcing $\delta F_0 = 0, \delta F_1 = 0$ in the unperturbed case, so that we can have the equilibrium mean state in $\left(\bar{U}_{\text{eq}}, \bar{\omega}_{\text{eq}}\right)$ in the unperturbed equilibrium. The beta-effect is taken as $\beta = 1$, and the topographic strength as $H = 3\sqrt{2}/4$ in (4.12). The first order linear control is considered here as in the general framework;

- We consider two parameter values $\mu = 2$ and $\mu = -0.5$. Usually the parameter μ defines the steady state mean flow $\bar{U} = -\beta/\mu$, thus this represents different directions in the large-scale mean jet. Especially when $\mu = -0.5$, there exists instability for the large-scale mean flow U due to topographic stress [32, 21];

- The perturbation is added in the large scale modes with $\delta F_0 = dF, \delta F_1 = dF$ in both test cases. The perturbation amplitude is taken as $dF = 1$. The goal in the control problem is to use the optimal control forcing $\vec{\kappa}(t)$ to drive the perturbed states back to the zero unperturbed mean.

The above parameter setup has been used as a stringent paradigm model in many previous problems [20, 16, 33].

As an illustration of the flow structure, we plot the mean stream functions and snapshots of flow vorticity for the two test regimes $\mu = -0.5$ and $\mu = 2$ in Figure 4.7. Both flow plots in unperturbed case $dF = 0$ and perturbed case $dF = 1$ are displayed, and the colormap is scaled into the same range for comparison. In the snapshots of the flow relative vorticity $\omega = \Delta\psi$, the perturbation forcing can induce stronger vortices in the perturbed vorticity field compared with weaker vortical modes in the unperturbed case. Also the full mean stream function $\bar{\Psi} = -\bar{U}y + \bar{\psi}$ combining the mean flow U and small-scale modes ψ is plotted to show the entire flow structure. It can be observed that the jets change directions in the two test cases $\mu = -0.5$ and $\mu = 2$. In the case with $\mu = -0.5$ (with eastward background mean steady flow $\bar{U}_{\text{eq}} = 1$), the unperturbed flow has strong jets in opposite directions in the mean stream function and the forcing perturbation tends to weaken the zonal jets. Conversely in the case with $\mu = 2$ (with westward background mean steady flow $\bar{U}_{\text{eq}} = -0.5$), the unperturbed case has a weaker jet while the perturbation forcing can generate strong opposite jets in both directions. These observations show the rapid changes in flow field structures and also in the flow statistics subject to the perturbations.

In the final verification step, we need to show the skill of the optimal control forcing achieved through the statistical control equations (4.13) and (4.17). The control forcing (κ_0, κ_1) is only applied on the mean flow state U and first vortical mode $\hat{\omega}_1$. Figure 4.8 and Table 1 display the percentage of statistical energy in unperturbed equilibrium in the two test cases. The large scale mean flow U always gets most of the energy (around 10% for $\mu = 2$ and 20% for $\mu = -0.5$) and then the ground modes $\hat{\omega}_{(1,0)}$ and $\hat{\omega}_{(0,1)}$. Still all the remaining modes in smaller scales which are not controlled count for more than 50 to 70 percent of the total statistical energy, thus are still important and crucial in the final flow structure. In the following control verifications, we will show whether we can control the responses due to interactions between various scales by only forcing the leading most energetic modes.

In running the barotropic model for statistical responses in mean and variance we can afford to run the model with an ensemble size $N = 1000$ for Monte-Carlo simulations using the 57-mode model, so that the essential statistics in the mean and variance can be captured with small error. Figure 4.9 displays the control results in the two test cases compared with the uncontrolled responses. In the beginning state the system is subject to the non-zero perturbation forcing δF at the largest scales U and ground mode ω_1, and the control forcing is added at time $T_{\text{ctrl}} = 5$ to drive the perturbed states back to statistical equilibrium. The figures show the responses in the mean flow U and the perturbed

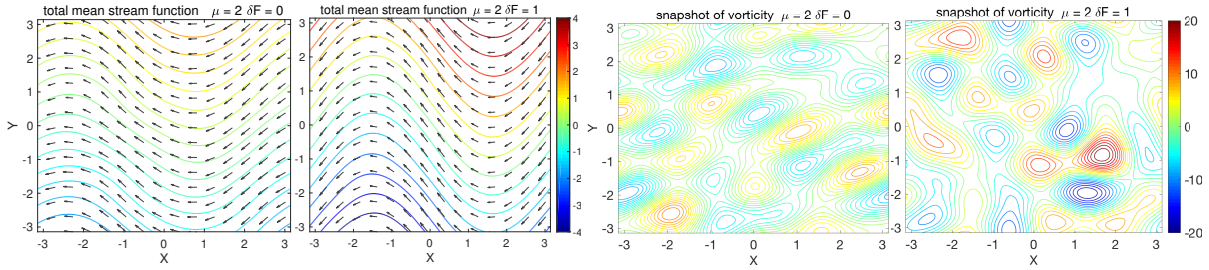

(a) mean stream function for $\mu = 2$

(b) snapshot of vorticity for $\mu = 2$

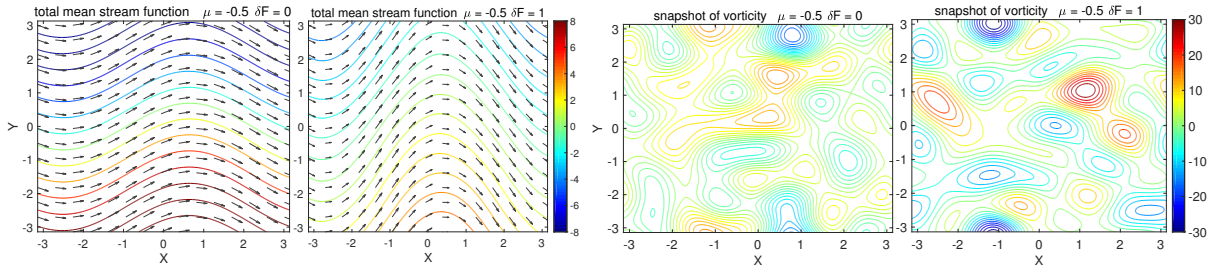

(c) mean stream function for $\mu = -0.5$

(d) snapshot of vorticity for $\mu = -0.5$

Figure 4.7: Mean stream functions $\bar{\Psi} = -\bar{U}y + \bar{\psi}$ with the vector flow field and snapshots of flow relative vorticity $\omega = \Delta\psi$ in the two parameter regimes $\mu = -0.5$ (eastward mean flow) and $\mu = 2$ (westward mean flow). Both the unperturbed case $dF = 0$ and perturbed $dF = 1$ case are shown. The colormap is scaled to the same range for comparison.

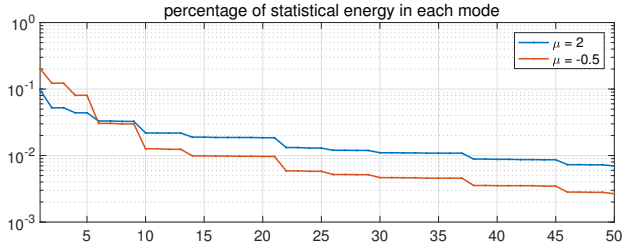

Figure 4.8: Percentage of statistical energy in each mode of the 57-mode model in descending order.

μ	U	$\hat{\omega}_{(1,0)}$	$\hat{\omega}_{(0,1)}$	$\hat{\omega}_{(1,1)}$	rest modes
-0.5	0.203	0.123	0.081	0.030	0.564
2	0.097	0.052	0.044	0.033	0.774

Table 1: Percentage of statistical energy in the leading modes of the 57-mode barotropic model.

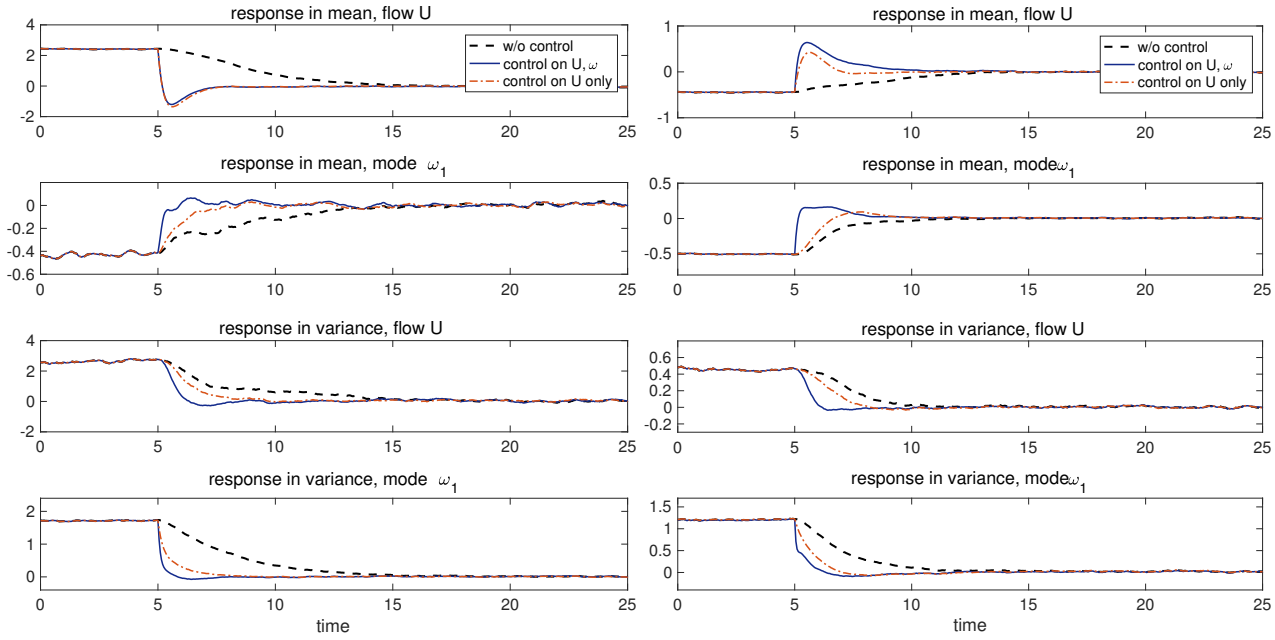

(a) $\mu = -0.5$ (b) $\mu = 2$

Figure 4.9: Control responses in regimes $\mu = -0.5$ and $\mu = 2$ with forcing perturbation in the mean state U and the topographic vorticity mode $\hat{\omega}_{(1,0)}$. Control is added at time $T_{\text{ctrl}} = 5$. The control results with control forcing on both mean flow U and first mode $\hat{\omega}_1$ (solid lines) and with control forcing only on the mean flow U (dotted-dashed lines) are compared with the responses without control forcing (dashed lines). The results are achieved through a Monte-Carlo simulation with ensemble size $N = 1000$ and with control parameter $\alpha = 0.05$.

modes ω_1, and the statistical mean and variance are calculated through an ensemble simulation of $N = 1000$ particles. Overall, the control forcing $\kappa(t)$ can effectively speed up the convergences of the perturbed states in both statistical mean and variance. For a further comparison about the control effects on each component, we also compare the performances of control forcing κ_0 only on the mean flow U and the full control κ_0, κ_1 on both the perturbed modes U, ω_1 as before. Obviously only controlling the mean flow U in this inhomogeneous flow field can be skillful but is insufficient to achieve the optimal control performance. Both mean and variance get slower convergence rates to the equilibrium state compared with the previous fully controlled results; and even the responses in the controlled direction U are not as good when no control forcing is applied on the other mode ω_1. This is due to the strong feedbacks from the vortical modes to the mean flow field through the topographic stress. Nevertheless the performance with control only on mean flow U is still better compared with the purely uncontrolled situation. To summarize, the statistical control strategy can offer an efficient way to develop the control forcing on the largest scales regardless of the high internal instability, but effectively drive the perturbed system back to equilibrium based on the total statistical energy structure.

For a further comparison, we also check the statistical energy responses in the unperturbed modes, $\sum_{|\mathbf{k}|^2 \geq 2} |\hat{\omega}_{\mathbf{k}}|^2$ in Figure 4.10. In this 57-mode model with a limited number of modes, the energy inside the small scale modes is small. Thus the responses in both the controlled and uncontrolled cases is equally small.

5. Summary

In this paper, we investigated a general statistical control strategy for complex dynamical systems with the help of a statistical energy conservation principle based on the framework first developed in [17]. The general turbulent systems of interest include a large group of universal models with energy-conserving nonlinearity. Instead of a direct control on the state variables in a high-dimensional phase space of the turbulent system with instability, we focus on a simple scalar dynamical equation developed in [15, 16] about the total statistical energy that combines the changes

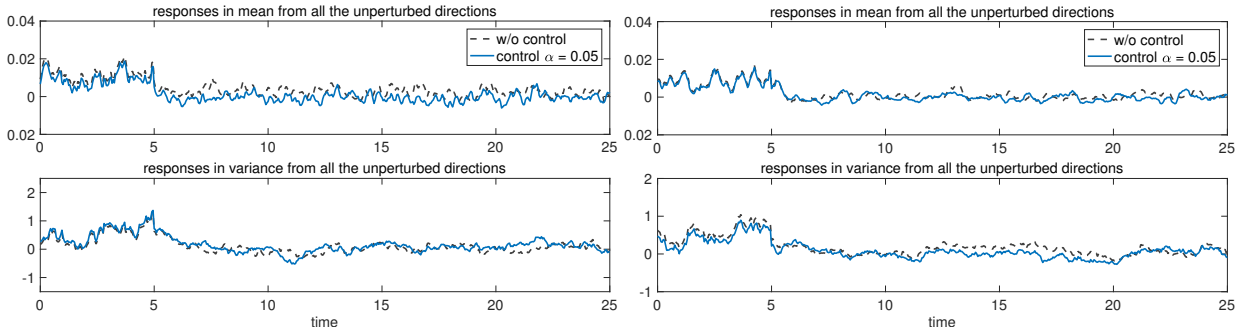

(a) $\mu = -0.5$ (b) $\mu = 2$

Figure 4.10: Control responses in the unperturbed modes $|\mathbf{k}|^2 \geq 2$ in regimes $\mu = -0.5$ and $\mu = 2$. The forced responses on these unperturbed modes are quite weak in these tests.

of energy in the mean and total variance. The total statistical energy equation offers an overall characterization of the statistical structure of the complex system related only with the deterministic forcing perturbation and statistical mean state, thus avoiding treating the complicated higher order nonlinear interactions with instability. The optimal control for this statistical equation is first solved with explicit solution by applying dynamic programming on the scalar statistical equation. Then in the second step the control forcing exerted on the original perturbed system can be recovered by inverting the achieved optimal statistical control related only with the first order mean statistical response of the system. In addition, the statistical responses in the mean subject to external forcing is approximated using linear response theory [23, 19] without the need to run the explicit model. In the two major mathematical tools used in the control method, the statistical energy principle relates the changes in total statistical energy with the perturbation in the first order mean state; and the mean responses are predicted with the linear response operator approximated by autocorrelation functions. The important advantage is that very little information is needed beforehand under this statistical control framework. Only the initial total changes in the statistical energy and a few autocorrelation functions of the target statistical steady state are required in finding the final form of control forcing without need of tracking the evolution of the full system and a large number of instabilities.

The control performance of this statistical strategy is then verified using two representative models involving inhomogeneity, that is, the 40-dimensional L-96 system and the topographic barotropic system including mean flow and small-scale interaction. The L-96 system can serve as a simple prototype model but can generate many representative statistical regimes. This enables us to compare the control performances in detail with different choices of model parameters in the simple setup of homogeneous perturbations. Then inhomogeneous perturbations are introduced in various small scale modes and the control skill is further confirmed. The barotropic flow topography offers another testbed for the anisotropic flow with various statistics. More detailed control forcing on a few large scale modes are required in this case to guarantee very effective statistical control. Despite the model errors introduced through the leading order expansion in both the statistical equation and linear prediction in mean response, the statistical control methods display uniform robust skill in all the numerical experiments for controlling the homogeneously and inhomogeneously perturbed system in the same fashion. The control forcing $\kappa(t)$ is found with high skill even admitting large errors in the statistical energy equation and mean response approximations. Furthermore this statistical control strategy shows potential for extremely high dimensional problems in turbulent flows and passive turbulence [16, 29]. Additional investigation is also required in strategies for finding the imperfect model parameters to achieve optimal performance in a systematic way, which in the present case is mostly determined empirically.

Acknowledgement

This research of the A. J. M. is partially supported by the Office of Naval Research through MURI N00014-16-1-2161 and DARPA through W911NF-15-1-0636. D. Q. is supported as a postdoctoral fellow on the second grant.

Appendix A. Statistical Control with Second-Order Responses in Inhomogeneous Perturbation

In the main text we always focus on the leading order expansion, $\bar{u}_{\rm eq}\cdot\delta F_0+\bar{F}_{\rm eq}\cdot\delta\bar{u}_0$, in the statistical control, while the second order responses, $\delta F_k\cdot\delta\bar{u}_k$, are assumed to be small or neglected in inhomogeneous perturbation cases. As one additional discussion we compare a more detailed control on the *second order statistical response* $\sum_k \delta F_k\cdot\delta\bar{u}_k$ with the previous homogeneous control only on the statistical mean in the main text.

Appendix A.1. Statistical control formulation with inhomogeneous perturbation in second-order response

We still consider the control problem through the statistical energy identity in the general form

$$\frac{dE}{dt}=-2dE\left(t\right)+C\left(t\right),\quad E\left(t_0\right)=E_0,\quad t_0\le t\le T. \tag{A.1}$$

In the same way, we use $C\left(t\right)$ for the total statistical control from the mean state perturbation. Notice that we can always include nonlinear terms inside the general statistical control functional $C\left(t\right)$ considering higher-order perturbations. Therefore an inhomogeneous control forcing $\vec{\kappa}\left(t\right)$ is introduced to control the system adaptively along each EOF in the controlled subspace $\{\mathbf{e}_k\}_{k=1}^M$

$$\bar{\mathbf{F}}_{\rm eq}=\bar{F}_{\rm eq}\mathbf{e}_0,\ \bar{\mathbf{u}}_{\rm eq}=\bar{u}_{\rm eq}\mathbf{e}_0,\quad \vec{\kappa}\left(t\right)=\kappa_0\left(t\right)\mathbf{e}_0+\sum_{k=1}^{M}\kappa_k\left(t\right)\mathbf{e}_k. \tag{A.2}$$

The generalized control is dependent on perturbation along each EOF direction

$$\begin{aligned} C\left(t\right)=C_0\left(t\right)+\sum_{k=1}^{M}C_k\left(t\right),\qquad & C_0\left(t\right)=\bar{u}_{\rm eq}\kappa_0\left(t\right)+\bar{F}_{\rm eq}\int_0^t\mathcal{R}_{\bar{u}}\left(t-s\right)\kappa_0\left(s\right)ds,\\ & C_k\left(t\right)=\kappa_k\left(t\right)\int_0^t\mathcal{R}_k\left(t-s\right)\kappa_k\left(s\right)ds. \end{aligned} \tag{A.3}$$

Above the leading order response in C_0 only contains *the linear homogeneous control* κ_0. Further we want to add individual controls κ_k along each smaller scale, thus *higher order nonlinear control* C_k needs also be considered. The cost function can be defined according to the equilibrium energy in each perturbed direction

$$\begin{aligned} \mathcal{F}_\alpha\left[C\left(\cdot\right)\right] &\equiv \int_t^T E^2\left(s\right)+\alpha\left(\sum_{k\neq0}w_k^{-1}C_k^2\left(s\right)ds+w_0^{-1}C_0^2\right)+k_TE^2\left(T\right),\\ v\left(x,t\right) &= \min_C\mathcal{F}_\alpha\left[C\left(\cdot\right)\right]. \end{aligned} \tag{A.4}$$

Above different penalty weight w_k should be added in each control mode C_k in the cost function $\mathcal{F}_\alpha$. We use the same strategy (2.18) in determining the control weight according to the equilibrium variance in each control direction. Each weight in small scales is proportional to the equilibrium variance in that direction, thus the more energetic modes get stronger control in response. In the control for the responses from uniform mean C_0 (which is responsible for the averaged feedback in the homogeneous state), the scaling is corresponding to the averaged one-point variance $r_{\rm 1pt}$. And all the weights are normalized. In this way, each component in cost function is balanced.

Following similar strategy in Section 2 of the main text, we can derive the optimal control equations for each control component

$$\begin{aligned} C_0^*\left(t\right)&=-\alpha^{-1}w_0K\left(t\right)E^*\left(t\right),\\ C_k^*\left(t\right)&=-\alpha^{-1}w_kK\left(t\right)E^*\left(t\right),\qquad 0\le t<T,\\ \frac{dE^*}{dt}&=-2dE^*\left(t\right)-\alpha^{-1}K\left(t\right)E^*\left(t\right). \end{aligned} \tag{A.5}$$

Since each spectral component in the cost function $\mathcal{F}_\alpha$ is weighted through the equilibrium variance w_k, the energy control in each mode is proportional to the ratio of equilibrium variance. The solution $K\left(t\right)$ of the scalar Riccati equation is exactly the same as the previous homogeneous case solution in (3.3), and the optimal energy control C_k

is consistent with the previous case by just replacing $\alpha_k = \alpha w_k^{-1}$. So the same exact solution can be applied. After solving the above equation for $K(t)$, exact same strategy can be applied for the control inversion along each direction of control $\kappa_k(t)$.

Now having achieved each component of the control parameter $C_k(t)$, the next problem is to recover the inhomogeneous control forcing $\vec{\kappa}(t)$ by inverting the nonlinear non-Markovian relation in (A.3). The control forcing in zero mode $\kappa_0(t)$ can be calculated using the same strategy as before in (2.21), thus the central problem is for new dynamical equations for the smaller scale forcing $\kappa_k(t)$. Still we use the linear approximation to estimate the autocorrelation functions. The linear response operator is approximated by autocorrelations with fitting parameters (γ_k, ω_k)

$$\mathcal{R}_k(t) = \exp\left[(-\gamma_k + i\omega_k)t\right].$$

Therefore we have the dynamical equations for the linear response $\mathcal{L}_k = \int_0^t \mathcal{R}_k(t-s)\kappa_k(s)\,ds$ under the linear model approximation of $\mathcal{R}_k$ in each mode

$$\frac{d\mathcal{L}_k}{dt} = (-\gamma_k + i\omega_k)\mathcal{L}_k(t) + \kappa_k(t), \quad 1 \le k \le M, \quad \mathcal{L}_k(0) = 0.$$

It needs to be noticed that small scale responses $\mathcal{R}_k, \mathcal{L}_k$ are both in complex values due to the phase parameter ω_k. The mean control forcing κ_0 can be recovered following exactly the same strategy as in the homogeneous case. Next we discuss the recovery of the nonlinear interactions due to small scale feedbacks.

Next we discuss about the inversion problem for the *quadratic* relation in complex values

$$C_k(t) = \kappa_k^* \mathcal{L}_k + \kappa_k \mathcal{L}_k^*, \quad \mathcal{L}_k = \int_0^t \mathcal{R}_k(t-s)\kappa_k(s)\,ds.$$

First note that the time derivative on the right hand side is real and can be calculated exactly as in the main text, $\dot{C}_k = \left(2d - K^{-1}\right)C_k$. Then it is easy to check the above nonlinear problem satisfy the following equation combining the linear regression model and nonlinear response

$$\begin{aligned}
\frac{d\kappa_k^r}{dt} &= -2C_k^{-1}\left[\left(\kappa_k^r\right)^2 + \left(\kappa_k^i\right)^2\right]\kappa_k^r + \left(\gamma_k + 2d - K^{-1}\right)\kappa_k^r - \omega_k\kappa_k^i, \\
\frac{d\kappa_k^i}{dt} &= -2C_k^{-1}\left[\left(\kappa_k^r\right)^2 + \left(\kappa_k^i\right)^2\right]\kappa_k^i + \left(\gamma_k + 2d - K^{-1}\right)\kappa_k^i + \omega_k\kappa_k^r.
\end{aligned} \tag{A.6}$$

Above in the spectral modes, $\kappa_k = \kappa_k^r + i\kappa_k^i$, we separate the dynamical equation for the complex control in real and imaginary parts. The initial value of the above system can be decided in the same fashion

$$\kappa_k^r(0) = \frac{\Re\mathrm{e}\delta\bar{u}_k(0)}{|\delta\bar{u}_k(0)|^2}C_k(0), \quad \kappa_k^i(0) = \frac{\Im\mathrm{m}\delta\bar{u}_k(0)}{|\delta\bar{u}_k(0)|^2}C_k(0). \tag{A.7}$$

Appendix A.2. Verification second-order control with inhomogeneous perturbation

Here we compare the performances of the control on second-order responses and the simple linear control model in the main text. We use the L-96 model with inhomogeneous forcing perturbations the same as Section 4.1. The most sensitive directions $k = 11, 12, 13, 14$ and the most energetic directions $k = 6, 7, 8, 9, 10$ are perturbed. The mean responses in the small scale modes using the homogeneous control forcing $\kappa_0(t)$ in main text and using the inhomogeneous control $\vec{\kappa}(t)$ above with forcing on the small scales are compared. In Figure A.1 the linear first-order control and the second-order control offer similar results in the responses in all the small scale modes. However, the second-order control method is in general much more expensive because the control forcing along each small scale modes needs to be calculated individually. As a result, the linear homogeneous control is sufficient to offer desirable control performance considering both efficient and effectiveness.

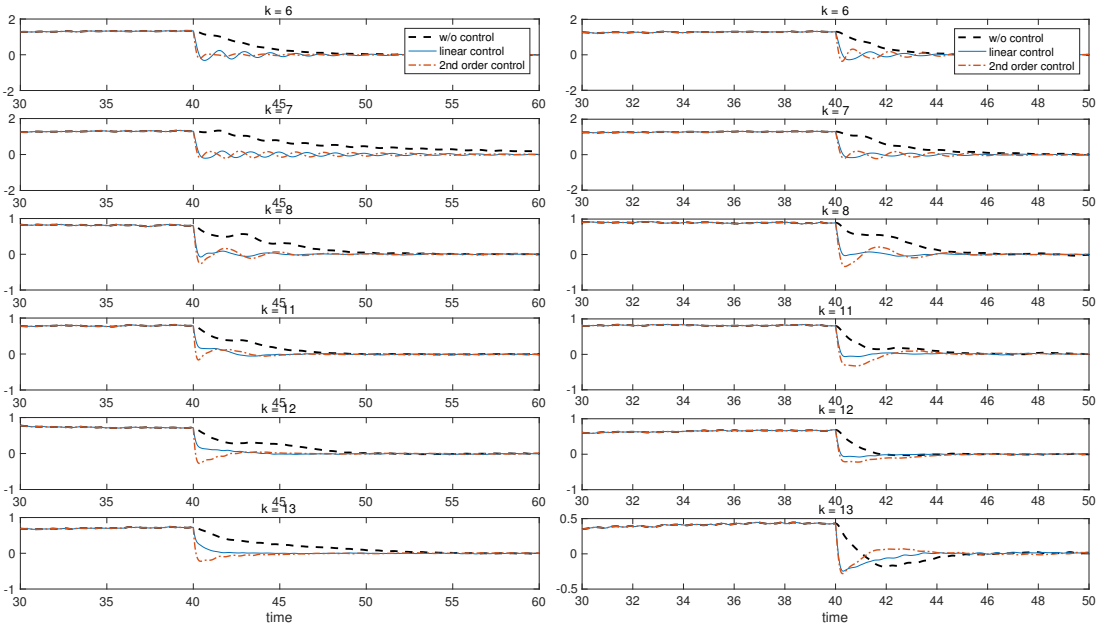

(a) responses in mean, $F = 6$

(b) responses in mean, $F = 8$

Figure A.1: Comparison of results with linear control and second-order control applied in L-96 system with inhomogeneous perturbations. The dashed black lines are the uncontrolled case; the blue lines are the case with leading order homogeneous control on the mean state; and the dotted-dashed red lines are the case with second-order control.

Appendix B. Information criterion for measuring autocorrelation functions of the stationary random fields

Here we propose one strategy in determing the optimal model parameter (d_M, ω_M) in Section 2.2.2 by fitting the lagged-in-time autocorrelation following the general method introduced in [28] with the help of information theory. A preferable measure to offer an unbiased metric for the imperfect model probability distribution π_M from the truth π is to use the relative entropy [22]

$$\mathcal{P}(\pi, \pi_M) = \int \pi \log \frac{\pi}{\pi_M}. \tag{B.1}$$

However one additional difficulty in tuning the autocorrelation functions under the information metric is that the autocorrelation functions is not actually a distribution function to measure in the relative entropy (B.1). The autocorrelation function $\mathcal{R}(t)$ may oscillate with negative values, thus it becomes improper to directly substitute $\mathcal{R}(t)$ into the formula (B.1) by replacing the distribution function π to measure the distance. The problem can be solved by instead considering the spectral representation of the random process $u(t)$, from the *theory of spectral representation* of stationary random fields [34]. It is proved by Khinchin's formula [34], that if the autocorrelation function $\mathcal{R}(t)$ makes smooth and rapid-decay, a positive definite matrix $E(\lambda) > 0$ can be constructed so that the *spectral representations* of the autocorrelation $\mathcal{R}(t)$ and stationary process u become

$$\mathcal{R}(t) = \int_{-\infty}^{\infty} e^{i\lambda t} dF(\lambda), \quad u(t) = \int_{-\infty}^{\infty} e^{i\lambda t} \hat{Z}(d\lambda), \tag{B.2}$$

where the spectral random measure $\hat{Z}(d\lambda)$ has independent increments and energy spectrum measured by $E(\lambda)$

$$dF(\lambda) = E(\lambda)\, d\lambda = \mathbb{E}\left|\hat{Z}(d\lambda)\, \hat{Z}^*(d\lambda)\right|.$$

Applying the theory for spectral representation of stationary processes, we find the one-to-one correspondence between the autocorrelation function $\mathcal{R}(t)$ and positive-definite energy spectra $E(\lambda)$. Back to the comparisons of

the true and model random fields u, u_M constrained within first two moments, $\mathcal{R}(t)$ for the true process u can be achieved through the data from true model simulations, while the imperfect model autocorrelation $\mathcal{R}_M(t)$ can be solved explicitly through the Gaussian linear process

$$du_M = -(d_M + i\omega_M) u_M dt + \sigma_M dW.$$

The autocorrelation function and corresponding spectral density function can be calculated in exact forms,

$$\mathcal{R}_M(t) = \exp(-(d_M + i\omega_M) t), \quad E_M(\lambda) = \int_{-\infty}^{\infty} e^{-i\lambda t} \mathcal{R}(t)\, dt = \frac{2d_M}{d_M^2 + (\lambda_M + \omega_M)^2}. \tag{B.3}$$

$E(\lambda)$ and $E_M(\lambda)$ then are the Fourier transforms of the autocorrelation matrices $\mathcal{R}(t), \mathcal{R}_M(t)$ according to (B.2). Therefore we can construct the spectral measures for two Gaussian random fields as a product of increment independent normal distributions about the frequency λ

$$\pi_G(x;\lambda) = \prod \mathcal{N}(0, E(\lambda)\, d\lambda), \quad \pi_G^M(x;\lambda) = \prod \mathcal{N}(0, E_M(\lambda)\, d\lambda).$$

The normalized relative entropy (B.1) between the two processes then can be defined under the spectral densities

$$\mathcal{P}\left(\pi_G, \pi_G^M\right) = \mathcal{P}(E(\lambda), E_M(\lambda)) \triangleq \int_{-\infty}^{\infty} \mathcal{P}\left(\pi_G(x;\lambda), \pi_G^M(x;\lambda)\right) d\lambda. \tag{B.4}$$

See [28] for a more detailed derivation about the above formula. Since E and E_M are positive definite for the spectral random variables, it is well-defined in the last part of the above formula (B.4) using the information distance formula (B.1). Through measuring the information distance in the spectral coefficients $\hat{Z}(d\lambda)$, we get the lack of information in the autocorrelation function $\mathcal{R}(t)$ from the model. Furthermore, we have shown in [28] that the error in autocorrelation functions $\|\mathcal{R}(t) - \mathcal{R}_M(t)\|$ of two stationary random processes u and u_M is bounded by the information distance of their energy spectra $\mathcal{P}(E, E_M)$.

To summarize, we can seek a spectral representation about the autocorrelation functions like

$$\mathcal{P}(E(\lambda), E_M(\lambda)) = \int \mathcal{D}\left(E(\lambda) E_M(\lambda)^{-1}\right) d\lambda, \tag{B.5}$$

where $\mathcal{D}(x) \equiv -\log\det x + \mathrm{tr}x - 2$ is the Gaussian relative entropy with a zero mean state. And since here we only concentrate on the leading order statistics (that is, mean and variance), thus this representation is enough. We can find the optimal model parameter $\boldsymbol{\theta}_* = (d_M, \omega_M)$ by minimizing the information metric defined in (B.5)

$$\mathcal{P}(E(\lambda), E_M(\lambda, \boldsymbol{\theta}_*)) = \min_{\boldsymbol{\theta}} \mathcal{P}(E(\lambda), E_M(\lambda, \boldsymbol{\theta})). \tag{B.6}$$

References

[1] D. G. MacMartin, B. Kravitz, D. W. Keith, A. Jarvis, Dynamics of the coupled human–climate system resulting from closed-loop control of solar geoengineering, Climate dynamics 43 (1-2) (2014) 243–258.

[2] D. G. MacMartin, K. Caldeira, D. W. Keith, Solar geoengineering to limit the rate of temperature change, Philosophical Transactions of the Royal Society of London A: Mathematical, Physical and Engineering Sciences 372 (2031) (2014) 20140134.

[3] S. L. Brunton, B. R. Noack, Closed-loop turbulence control: progress and challenges, Applied Mechanics Reviews 67 (5) (2015) 050801.

[4] M. B. Horowitz, A. Damle, J. W. Burdick, Linear Hamilton Jacobi Bellman equations in high dimensions, Decision and Control (CDC), 2014 IEEE 53rd Annual Conference on. IEEE (2014) 5880–5887.

[5] Y. T. Chow, J. Darbon, S. Osher, W. Yin, Algorithm for overcoming the curse of dimensionality for time-dependent non-convex Hamilton–Jacobi equations arising from optimal control and differential games problems, Journal of Scientific Computing (2016) 1–27.

[6] B. D. Anderson, J. B. Moore, Linear optimal control, Vol. 197, Prentice-Hall Englewood Cliffs, NJ, 1971.

[7] M. Bardi, I. Capuzzo-Dolcetta, Optimal control and viscosity solutions of Hamilton-Jacobi-Bellman equations, Springer Science & Business Media, 2008.

[8] L. C. Evans, An introduction to mathematical optimal control theory, Lecture Notes, University of California, Department of Mathematics, Berkeley.

[9] R. Bellman, Dynamic programming, Princeton University Press 89 (1957) 92.

[10] J. Kim, T. R. Bewley, A linear systems approach to flow control, Annu. Rev. Fluid Mech. 39 (2007) 383–417.

[11] D. R. Nicholson, Introduction to plasma theory, Cambridge Univ Press, 1983.
[12] R. Salmon, Lectures on geophysical fluid dynamics, Oxford University Press, 1998.
[13] S. B. Pope, Turbulent flows, IOP Publishing, 2001.
[14] T. T. Medjo, R. Temam, M. Ziane, Optimal and robust control of fluid flows: some theoretical and computational aspects, Applied Mechanics Reviews 61 (1) (2008) 010802.
[15] A. J. Majda, Statistical energy conservation principle for inhomogeneous turbulent dynamical systems, Proceedings of the National Academy of Sciences 112 (29) (2015) 8937–8941.
[16] A. Majda, Introduction to turbulent dynamical systems in complex systems, Springer, 2016.
[17] A. J. Majda, D. Qi, Effective control of complex turbulent dynamical systems through statistical functionals, Proceedings of the National Academy of Sciences 114 (22) (2017) 5571–5576.
[18] E. N. Lorenz, Predictability: A problem partly solved 1 (1).
[19] A. J. Majda, D. Qi, Improving prediction skill of imperfect turbulent models through statistical response and information theory, Journal of Nonlinear Science 26 (1) (2016) 233–285.
[20] D. Qi, A. J. Majda, Low-dimensional reduced-order models for statistical response and uncertainty quantification: barotropic turbulence with topography, Physica D: Nonlinear Phenomena 343 (2016) 7–27.
[21] A. Majda, X. Wang, Nonlinear dynamics and statistical theories for basic geophysical flows, Cambridge University Press, 2006.
[22] A. Majda, R. V. Abramov, M. J. Grote, Information theory and stochastics for multiscale nonlinear systems, Vol. 25, American Mathematical Soc., 2005.
[23] A. J. Majda, B. Gershgorin, Y. Yuan, Low-frequency climate response and fluctuation–dissipation theorems: theory and practice, Journal of the Atmospheric Sciences 67 (4) (2010) 1186–1201.
[24] M. Hairer, A. J. Majda, A simple framework to justify linear response theory, Nonlinearity 23 (4) (2010) 909–922.
[25] C. Leith, Climate response and fluctuation dissipation, Journal of the Atmospheric Sciences 32 (10) (1975) 2022–2026.
[26] A. Gritsun, G. Branstator, Climate response using a three-dimensional operator based on the fluctuation–dissipation theorem, Journal of the atmospheric sciences 64 (7) (2007) 2558–2575.
[27] A. Gritsun, G. Branstator, A. Majda, Climate response of linear and quadratic functionals using the fluctuation–dissipation theorem, Journal of the Atmospheric Sciences 65 (9) (2008) 2824–2841.
[28] D. Qi, A. J. Majda, Predicting fat-tailed intermittent probability distributions in passive scalar turbulence with imperfect models through empirical information theory, Comm. Math. Sci 14 (6) (2015) 1687–1722.
[29] D. Qi, A. J. Majda, Predicting extreme events for passive scalar turbulence in two-layer baroclinic flows through reduced-order stochastic models, Comm. Math. Sci, in press.
[30] G. K. Vallis, Atmospheric and oceanic fluid dynamics: fundamentals and large-scale circulation, Cambridge University Press, 2006.
[31] J. G. Charney, J. G. DeVore, Multiple flow equilibria in the atmosphere and blocking, Journal of the atmospheric sciences 36 (7) (1979) 1205–1216.
[32] G. F. Carnevale, J. S. Frederiksen, Nonlinear stability and statistical mechanics of flow over topography, Journal of Fluid Mechanics 175 (1987) 157–181.
[33] A. J. Majda, I. Timofeyev, E. Vanden-Eijnden, Systematic strategies for stochastic mode reduction in climate, Journal of the Atmospheric Sciences 60 (14) (2003) 1705–1722.
[34] A. M. Yaglom, An introduction to the theory of stationary random functions, Courier Corporation, 2004.